ADDIS ABABA UNIVERSITY

ADDIS ABABA INSTITUTE OF TECHNOLOGY

AFRICAN RAILWAY CENTER OF EXCELLENCE

PERFORMANCE OF PRESTRESSED CONCRETE SLEEPERS UNDER STATIC LOADING

A Thesis in Railway Engineering (Civil Infrastructure)

By Mujawimana Violette

October, 2021

A Thesis submitted in Partial Fullfillment of the Requirements for the Degree of Master of Science in Railway Engineering (Civil Infrastructure)

DECLARATION

I certify that research work titled "**Performance of Prestressed Concrete Sleepers under Static Loading**" is my own work. The work has not been presented elsewhere for assessment. Where material has been used from other sources it has been properly acknowledged.

Signed: …… Date…

MUJAWIMANA Violette

violettemujawimana@gmail.com

APPROVAL

The undersigned have examined the research work entitled **'Performance of Prestressed Concrete Sleepers Under Static Loading** presented by

MUJAWIMANA Violette of registration number GSR/5163/12, a candidate for the degree of Master of Science in Railway Engineering (Civil Infrastructure) and hereby certify that it is worth of acceptance.

Dr. Abrham Gebre		
Advisor	Signature	Date
Mr. Zewdie Moges		
Internal Examiner	Signature	Date
Dr-Ing. Adil Zekaria		
External Examiner	Signature	Date
Mr.Zewdie Moges		
Chair person	Signature	Date

ABSTRACT

Railway pre-stressed concrete sleepers are an integral part of the railway track as they hold and move the wheel loads from the rails to the track foundation. Prestressed concrete sleepers are subjected to various types of static load condition after a certain time, which can lead to some reduction in the effective behaviour of sleepers. Consequently, in order to preserve efficiency and to prevent the degradation of the railway system, it is important to consider various conditions of support during the design of the railway sleepers. The objective of this research was to study the load-carrying capacity of the prestressed concrete sleepers where Polybeam and BOEF were used for flexural analysis and a Finite element package ABAQUS was used to analyse the static loading response on prestressed concrete sleepers considering elastic support. From flexural analysis, at the rail seat the results have shown that the maximum bending from Polybeam and maximum bending moment from BOEF the percentage difference is 0.19% and at the center of the sleeper the maximum bending moment from BOEF and maximum bending moment from Polybeam the percentage difference is 5.12%. The maximum shear force at rail seat the results have shown that maximum shear force from BOEF and maximum shear force from Polybeam are similar because the percentage difference is 0.01%.For deflections for rail seat and at the center of the sleeper the results have shown that the percentage difference is 4.9% and 5.47% respectively. Therefore there is a small portion of difference between results from Polybeam and BOEF.From static modeling, the possible favorable and unfavorable elastic support circumstances have been analyzed. With a lot of variance in ballast rigidity and very soft support underneath the center of the sleeper and along the length of the sleeper, for all circumstances the results show that the displacements and stresses are significant on the rail seat and it has shown that onceballast stiffness reduce at the centre of the sleeper from 100% to 90%,80%.70%,60%,50%,40%.30%, 20%, and 10% supported , the displacement of the sleeper increased a small portion of (0.004%-0.091%) more than 100% supported and stresses increased(0.027%-0.07%) more than 100% supported. Therefore, once the ballast stiffness reduces at the center of the sleeper there is a small increase in displacement and stresses but to keep the performance of the sleeper, the low ballast stiffness at the center of the sleeper should be avoided. once the ballast stiffness reduce along the sleeper from 100% supported (full supported) to 90% , 80%, 70%, 60%,50% and 25% supported , the displacement increased with 3.27%, 7.29%, 12.37%, 18.97%, 27.94% and 76.7% respectively more than full supported and von mises stresses increased 0.28%, 0.86%, 1.06%, 1.062%, 3.12% and 12.04% respectively more than 100% supported . Therefore, when there is high ballast stiffness reduction along the sleeper, there is more increasing in displacement. Because it is impossible to predict the exact support distribution, it is of importance for sleeper designers and manufacturers to evaluate the influence of variations in ballast stiffness and distribution.

Keywords: *prestressed concrete sleepers, static loading, elastic full support and partial support, Abaqus*

ACKNOWLEDGMENTS

First and foremost, I want to thank God for his protection through this research.

I would like to express my deepest appreciation to Dr. Abraham Gebre, my research advisor for his advice, and guidance, he offered in this thesis work.

I would also like to express my gratitude to the lecturers who assisted us throughout the two semesters of coursework. Special thanks to IUCEA through African Railway Center of Excellence (ARCE) for all the given financial supports during my study of Master of Science program in Addis Ababa University.

Unlimited gratitude goes to my family, especially my husband BITWAYIKI Jean Paul and my son MUGISHA SHEMA Aime Tresor for the unlimited support and encouragements.

Finally, I would like to thank Almighty God for helping me and being with me during my studies and my stay in Ethiopia.

TABLE OF CONTENTS

LIST OF FIGURES

LIST OF TABLES

LIST OF ABBREVIATIONS

Term	Meaning
AALRT	Addis Ababa Light Rail Transit
ARCE	African Railway Center of Excellence
AREA	American Railway Engineering association
AREMA	American Railway Engineering and Maintenance-of-Way Association
AS	Australian Standard
BOEF	Beam On Elastic Foundation
CAD	Computer Aided Design
ERC	Ethiopian Railway Corporation
FEA	Finite Element Analysis
FEM	Finite Element Method
FFU	Fiber-reinforced foamed Urethane
LRT	Light Rail Transit
LST	Livermore Software Technology
PC	Prestressed Concrete
PCSs	Prestressed Concrete Sleepers
RSD	Rail Seat Deterioration
UK	United Kingdom (Great Britain and Northern Ireland)
USA	United State of America
USP	Under Sleeper Pads

LIST OF NOTATION AND DEFINITIONS

Notation	Definitions
μ_c	concrete Poisson's ratio
μ_s	Steel Poisson's ratio
ρ_c	Concrete Density
α_c	Concrete Thermal expansion coefficient
ε_c	Compressive strain in the concrete
ε_{c1}	Compressive strain in the concrete at the peak stress
ε_{cu}	Ultimate compressive strain in concrete
ε_u	Strain of reinforcement or prestressing steel at maximum load
f_{plk}	Characteristic strength of steel
f'_c	Characteristic strength of concrete
f'_{ct}	Tensile strength of concrete
f_{cd}	Design value of concrete compressive strength
f_c	Compressive strength of concrete
f_{ck}	Characteristic compressive cylinder strength of concrete at 28 days
f_{ctk}	Characteristic axial tensile strength of concrete
E	Young's modulus
E_c	Concrete Young's modulus
E_s	Steel Young's modulus
B	Sleeper width
K_S	Total ballast stiffness under sleeper
K_1-K_3	Ballast stiffness for each part of sleeper
P_t	Prestressing force
A_p	Area of steel wires
A_g	Gross area of cross-section
ULS	Ultimate limit state

Chapter 1: INTRODUCTION

1.1 Background

Transportation systems play a significant role in each country's economic and social development. The rail system is one of the most effective transport networks that is ideal for long and short distances [1].

Railway track consists of elements of the substructure and superstructure. The sub-structure consists of various layers, such as ballast, subballast and subgrade, and the upper portion is the superstructure that includes sleepers, rail pads, fasteners and rails. Sleepers are components of the railway track that rest transversely on the ballast layer and provide stability and retain the gauge where the stresses are transferred to granular material [1]. According to A. Parvez and S. J. Foster sleepers have been used in the railway sector for over 50 years and they can be manufactured using timber, concrete, steel, or other engineering materials. According to Ruilin You , et al. concrete is commonly used around the world and it is required to check the validity for sleepers in order to maintain the good performance of railway geometry [2].

Many approaches for pre-stressed concrete sleepers have been developed and tested. Monobloc pre-stressed concrete sleepers are the most often used among these. Due to their weight advantage, twin-bloc sleepers are also gaining popularity. Twin-block sleepers are made comprised of two concrete components that are joined together by steel reinforcing [3].

In research made by Y. Panga, et al repeating wheel loads may cause the bad performance of the ballast material, which would affect the support conditions beneath the sleepers. Therefore, understanding the influence of different support conditions on the degradation of sleepers is necessary for maintaining safe railroad operations [4]. Another issue caused by ballast subsidence is the formation of a gap between the sleeper and the ballast, resulting in the suspension or partial suspension of the sleepers over the settlement ballast. It was often found that the sleepers hang from the rails at railway sites and the unsupported sleeper is often referred to as " the hanging sleeper'[6] Therefore, the support condition of railway sleepers has a major impact on the mechanical efficiency and actions of sleepers and railway tracks and one of the important issues in this regard relates to current unsupported sleepers on railway tracks [5].The finite element analysis in this research has presented the numerical analysis of Prestressed Concrete Sleepers under static loads considering different support conditions by using ABAQUS as numerical model.

1.2 Problem Statement

Prestressed concrete sleepers are among major components of railway track as their main function is to carry and transfer the wheel loads from the rail to the granular material and to hold the rails to gauge.Therefore, due to extensive increases in axle loads, speed and traffic volumes in rail transport systems; this is needed to provide a more detailed understanding of the behaviour of the prestressed concrete sleepers to ensure their efficiency [6].

Vertical static forces have been the main subject of study, since they are the main cause of poor railway sleepers efficiency due to static axle loads [7].

A limited number of researchers considered the support conditions and it was that inadequate sleeper support conditions were found to be a critical factor leading to the reduction of comfort and accidents. Also, the ballasts as the support of the sleeper may not provide adequate support in the field conditions due to numerous load conditions and may provide ineffective support for the sleeper, so it is important to anticipate bending moments along the sleepers. Therefore, in this research numerical analysis of Prestressed Concrete Sleepers under Static loads was conducted with different support conditions

1.3 Research Objectives

1.3.1 General objective

The main objective of this study is to study the Performance of Prestressed Concrete Sleepers under Static Loading

1.3.2 Specific Objectives

1. To review the flexural analysis of monoblock prestressed concrete sleeper
2. To analyse the effect of ballast reaction reduction on flexural capacity of prestressed concrete sleepers
3. Static modeling of monoblock prestressed concrete sleeper with elastic support conditions

1.4 Methodology

The existing literature on related topics in the library, and reports, books, journals and other publications, research paper and sources available in electronic media were reviewed. The basic design parameters and input data were identified and conducted from Ethiopian Railway Corporation (ERC) as some input data; and from different foreign standards like AS1085.14, AREMA, Chinese Standard and other acknowledge publications used in the design of pre-stressed concrete sleeper. Generally, the following was followed in this research.

- Input parameters which are obtained from ERC, AREMA, Chinese standard, Australian Standard (AS) and other acknowledged publications were used to review the design of a monoblock concrete sleeper where flexural moments, shear forces and deflections were calculated by using Polybeam Software with different ballast reaction distribution.
- For Numerical model ABAQUS software was used and based on numerical analysis, one monoblock prestressed concrete sleeper with different support distribution and with material properties of concrete and steel such as density, Young's Modulus, Poisson ratio were put in model where static structural analysis conducted to study the prestressed concrete sleepers response (Stresses and deformations) under elastic support

The detailed methodology on Numerical model was shown in figure 1.1

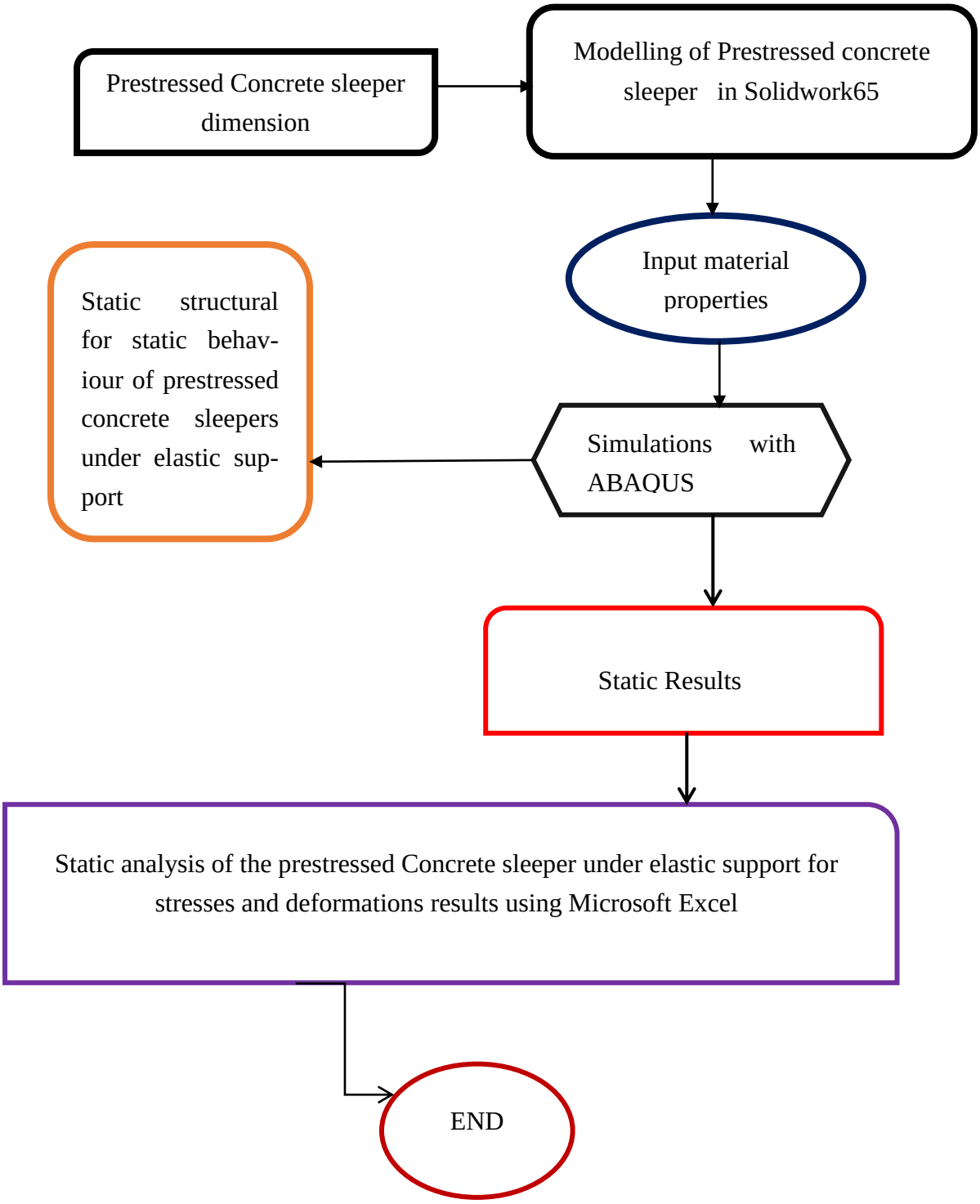

Figure 1.1 A Flow Chart of the Methodology

1.5 Scope and Limitations of the Thesis

The research has focused on numerical analysis of prestressed concrete under static loads. Flexural capacity of prestressed concrete has been conducted and numerical static simulation was developed as a suitable way to develop an understanding of the static behavior of PCs sleepers. Only, the vertical wheel load was considered, and elastic support was considered as support condition, the other track loadings were not considered. The effect of other track components, like rail pads, ballast bed and subgrade, and the experimental investigations were not conducted in this research. Therefore, only numerical simulations were conducted.

1.6 Organization of the Thesis

This Thesis is presented in 5 chapters as follows:

- Chapter 1 gives a brief background and the problem statement of the research. The objective, the scope, and the research methodology and limitations to the research are found in this chapter.

- Chapter 2 Literature Review where the behavior of Prestressed Concrete Sleepers (PCSs) under static loading has been reported. Some numerical modeling using finite element packages of PCSs were also discussed.
- Chapter 3 describes the design of a concrete sleeper with Polybeam as software for analysis where flexural moments in the sleeper (positive at rail seat and negative at the center) were statically calculated. Finite Element Modeling as methodology used for Static simulation was also discussed and the validation of FEM was shown in this chapter. .

- Chapter 4 presents the analysis results and discussion: this part contains the numerical analysis result of studied sleepers. The deformations and stresses were presented and discussed.
- Chapter 5 Conclusion and recommendations. In the final chapter, the research thesis has been concluded and further research areas have been suggested.

Chapter 2: LITTERATURE REVIEW

2.1 Railway Track

The track on a railway or railroad, also known as the permanent way, is the structure that includes the rails, fasteners, railroad ties, ballast (or slab track), and the subgrade beneath. It enables trains to travel by providing a stable surface on which their wheels can roll on [8].

2.1.1 Railway Track Structure Components

In compliance with M. A. Sayeed and M. A. Shahin transportation industry has a major drive for every country around the world to expand both the economy and society. It is generally understood that the railway system now offers the easiest and safest option for either passenger or freight transportation [9].

Recent increases in passenger and freight traffic have resulted in more extensive use of many railway routes than ever before, with a consequent need for more regular maintenance of tracks. The bulk of the railways in the world are on ballast lines. The existing asset volume is such that the dominance of ballast track is unlikely to change, while new railways may be constructed using slab track [10].

The track is subdivided into two major groups: superstructure and substructure. A category known as the superstructure is composed of visible track components such as rails, rail pads, concrete sleepers, fastening systems, under sleeper pads, and ballast as shown in Fig 2.1. The substructure is associated with a sub-ballast, ballast mat and sub-grade geotechnical framework [11].

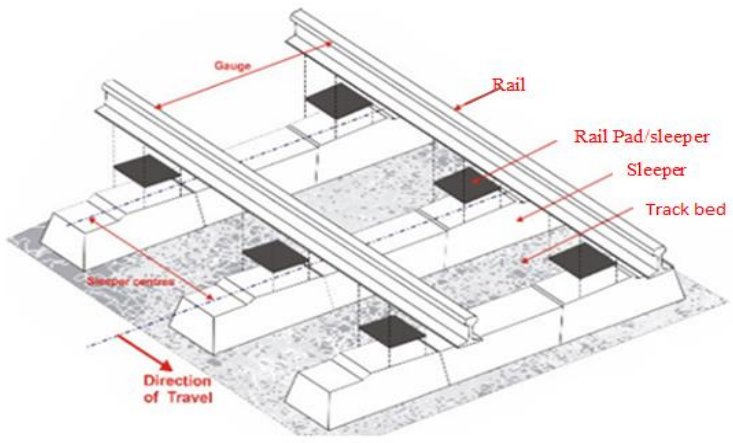

Figure 2.1 Cross section of a railway track [11]

2.1.1.1 Railway track Superstructure Components

***Rails*:** Rails are the longitudinal steel members that direct the train wheels in an even and continuous manner. They must be stiff enough to act as beams, transferring concentrated wheel loads to spaced sleeper supports without excessive deflection between them [12].

The rail fastening is the system that secures the rails to the sleepers; it prevents the rails from rotating, provides elasticity to the track, and dampens the transmission of noise and vibrations to the infrastructure when trains pass. These can be composed of different materials, namely, plastic, rubber or metal. Under in-service conditions, the loading amplitude and frequency of the rail pads depends on the speed and axle-load of the train running on the track [13].

Sleepers: sleepers are the primary structural elements of a railway track. Sleepers are responsible for ensuring track gauge, ensuring lateral stability of the track, and contributing to better geometrical conditions of the track, in addition to pressure distribution and load transfer to the underlying layers. sleepers are subjected to vertical, lateral, and axial forces**.** [14].

2.1.1.2 Railway Track Substructure Components

Ballast : ballast bed plays a significant role to provide resistances during train operation, provide a hard and level bed for sleepers hold sleepers in place during passage of trains ,transfers and distributes load from sleepers to larger area , provides effective drainage and Prevent vegetation growth and Provide track stability [15].

***Subballast*:** sub ballast is layer, which serves between ballast layer and subgrade layer and composed of much finer particles than the upper ballast. It works as a filter which on the one hand prevented the mutual penetration between ballast and soft soil subgrade and thickness of the gravel sub-ballast layer is 15 cm. Ballast layer are not normally used in some railways project and they simply use a greater thickness of the formation layer, which is placed on top of the subgrade [16].

Subgrade: Subgrade is the foundation of the track structure and its primary function of the subgrade is to provide a stable foundation for the track structure. The degree of compaction, moisture content, and soil type all have an impact on its load bearing capacity. A useful subgrade is one that can withstand a high level of loading without deforming significantly [17].

2.1.2 Railway track forces

The track system forces are usually divided into three groups depending on their existence, which are static forces (usually induced by vehicle body mass) Quasi-static loads (or dynamic ride loads) associated with vehicle motions and dynamic (dynamic wheel/rail) forces associated with significant irregularities that may occur during the life of the track system [17].

2.1.2.1 Static forces on track

Vertical forces

Vertical forces include dead loads, dynamic augment of loads such as the effect of speed, the hammer blow effect, the inertia of reciprocating masses, and forces perpendicular to the plane of the rails, the actual direction of which is determined by track cross-level and grade, as well as vertical wheel and uplift forces [18].

Vertical wheel force

The vertical wheel force is often simplified as a static component equal to the vehicle weight divided by the number of wheels. On moving trains, combining this vertical wheel force with track geometry, vehicle dynamics and/or rail and wheel conditions can produce variety of dynamic forces [19].

Uplift forces

Figure 2.2 describes the reaction of a rail to a vertical load at the wheel contact points; the rail tends to lift up, drifting away from the wheel. If the weight of the sleeper and rail, as well as ballast confinement (frictional force), do not counteract this uplift force, the sleeper will raise suddenly. This movement causes a pumping action on the track bed, which can cause track components to deteriorate if it sits on cohesive soils or fully fouled ballast [20].

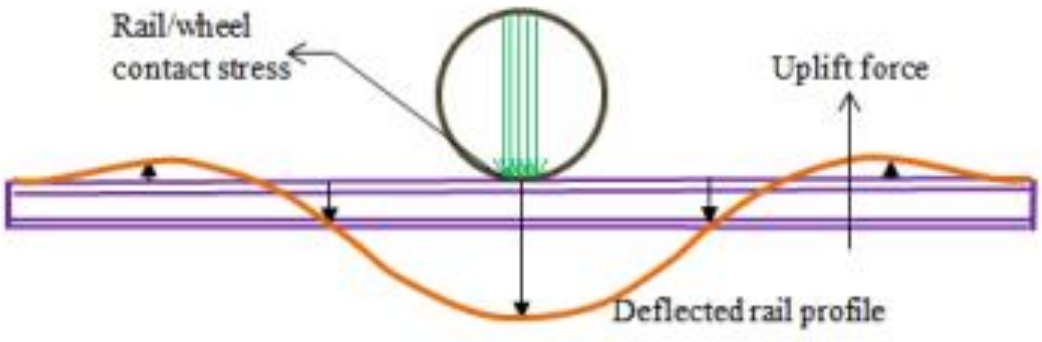

Figure 2.2 An illustration of uplift force occurrences [21]

Lateral force

The forces in lateral direction act on the track structure, parallel to the long axis of the sleepers, usually comes from the lateral wheel force due to the friction between the rail and wheel especially when a train goes around corners. It also comes from the buckling reaction force of the rail, which is usually caused, by a high longitudinal force in the rail [22].

Longitudinal forces

The forces in longitudinal direction act on the track structure, parallel to the rails. It is usually due to acceleration and braking of trains and thermal expansion or contraction of the rails [23]

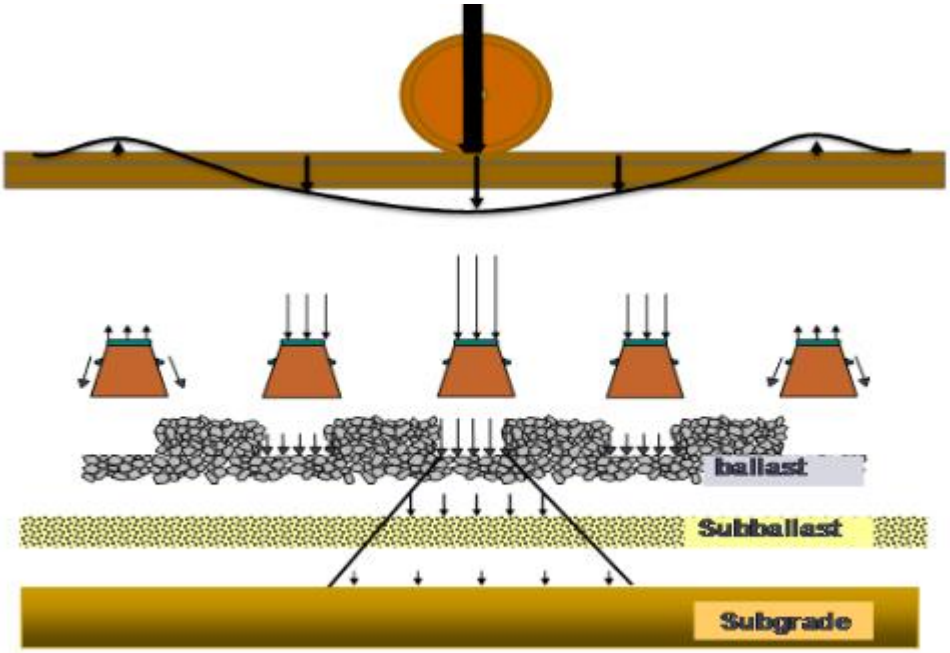

Figure 2.3 Typical wheel load distribution into the track structure [24]

2.2 Sleepers

Railway sleepers are an essential part of railway track design. Its primary aim is to distribute loads from the rail foot to the underlying ballast bed and maintaining the gauge. Based on the materials used for sleeper construction, they are classified as wooden sleepers, steel sleepers, cast iron sleepers, R.C.C sleepers, and pre-stressed concrete sleepers [25].

2.2.1 Concrete sleepers

Actually, concrete was manufactured with just three ingredients: cement, aggregate, and water; the cement was usually Portland cement, as stated in. Soon, very small amounts of chemical products were applied to the mix to enhance some of the properties of concrete, either in the fresh or hardened condition [26].

In compression, concrete is solid, but in stress it is weak. Concrete is more elastomeric than plastic. Regardless of the concrete's thickness, the ultimate strain for most structural concretes is approximately 0.0035 [27].

The elastic deformations of concrete largely depend on its composition (especially the aggregates). From Eurocode 2 [28] the modulus of elasticity of a concrete is controlled by the moduli of elasticity of its components. Approximate values for the modulus of elasticity E_{cm} , secant value between σ_c = 0 and O.4f_{cm}, for concretes with quartzite aggregates, for limestone and sandstone aggregates the value should be reduced by 10% and 30% respectively. For basalt aggregates, the value should be increased by 20% [29].

The value of the design compressive strength is given by

$$f_{cd} = \alpha_{cc} f_{ck} / \gamma_c \qquad 2.1$$

where: γ_c is the partial safety factor for concrete, , and α_{cc} is the coefficient taking account of long term effects on the compressive strength and of unfavourable effects resulting from the way the load is applied.

Where the tensile strength is determined as the splitting tensile strength, $f_{ct,sp}$, an approximate value of the axial tensile strength, $f_{ct,}$ may be taken as

$$f_{ct} = 0.9 fct, sp \qquad 2.2$$

Where

f_{ct} is tensile strength of concrete ,$f_{ct,\,sp}$ is splitting tensile strength of concrete

Precast concrete should not be too heavy or too thin for better quality, and it should be of moderate weight for ease of handling. The specification should be written in such a way that the gauge, track alignment, and rail levels can be easily changed and maintained.

According to Shan [30] , the use of prestressed 60MPa concrete, the sleepers can be able to tolerate a wide variety of loading conditions .Furthermore, minor cracks that may occur due to unintentional damage close immediately, preventing the reinforced steel from rotting and any damage to the sleepers' reputation.

2.2.1.1 Prestressed Concrete Sleepers

In particular, since last 50 years, railway pre-stressed concrete sleepers have been used in the railway industry [31].

Prestressed concrete are sleepers that resist flexure by using concrete and prestressing tendons and are important for the structural integrity of railway track structures, transferring wheel loads from the rails to the underlying ballast bed, while securing rail gauges for safe train traffic and they have an improved structural capacity and serviceability as compared to conventional reinforced concrete. Given their importance, it is crucial to ensure that concrete sleepers are always in excellent condition before and during operation [32].

PSCs are expected to have a longer life cycle, lower maintenance costs than other concrete sleepers and structures, and to withstand static and high dynamic loads as well as harsh environments. Because of their durability and long-term performance, they rely heavily on creep and shrinkage responses [33].

Concept of Prestressing

The application of an initial load on a structure before it is used is known as the initial load. The initial load, also known as "pre-stress," is applied to allow the structure to withstand the stresses that arise during its service life. Pre-stressing a structure is not the only way to do it. Pre-stressing was a term that existed before actual implementations [34].

Prestressing is applied to concrete by means of high-strength tendons (usually steel) in tension, passing through the concrete. This can be accomplished in one of two ways: pretensioning and posttensioning, with the main difference being whether the steel is tensioned then when the concrete is cast, hence the terms pre and post [35].

Full prestressing and partial prestressing are the two types of prestressing. Prestressing in which sufficient precompression is used to ensure crack-free performance at full design load, and partial prestressing in which precompression is insufficient to prevent cracks at full design load. As a result, the member will typically include some conventional reinforcement bars [35] [36].

The following stages are involved in pre-tensioning

1) Anchoring of tendons against the end abutments
2) Placing jacks
3) Applying tension to the tendons
4) Casting of concrete
5) Cutting of the tendons

The initial load or 'pre-stress' is applied to enable the structure to counteract the stresses arising during its service period

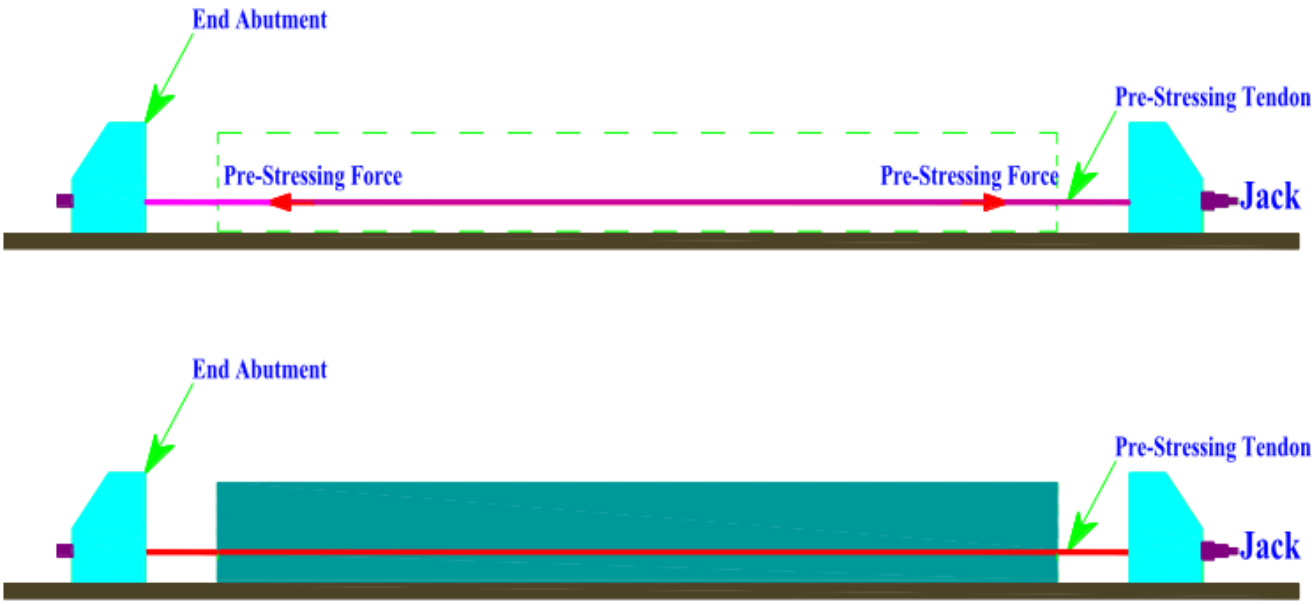

Figure 2.4 Stages of pre-tensioning [35]

2.2.1.1 .1 Monoblock Prestressed concrete sleepers

Prestressed mono-block concrete sleepers can be produced by using individual moulding . When prestressing is transferred to concrete via bonds and positive anchorages in the case of pre-tensioned sleepers or only via positive anchorages in the case of post-tensioned sleepers, this method is typically used. The pre-tensioned type mould is designed to withstand the initial prestressing force and must thus be stronger than moulds used in other systems [36].

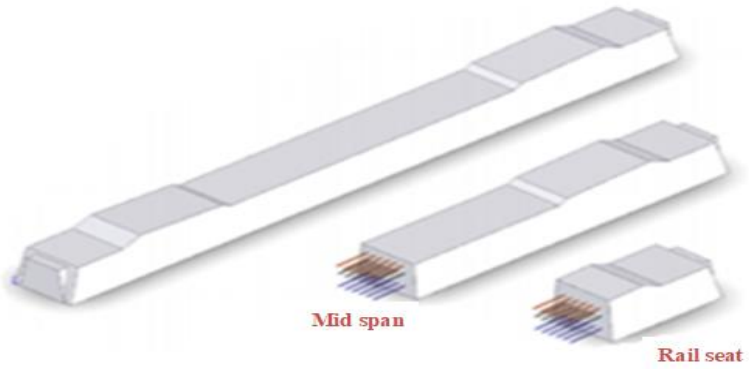

Figure 2.5 A monoblock prestressed concrete sleeper cross-section [37]

2.2.1.1.2 Two-block sleepers

Bi-block sleepers are made up of two concrete rail supports connected by steel where blocks are joined by transverse steel T bar and they are pretensioned but not reinforced. They have a design that flexes and behaves similarly to wood ties.

Pre-tensioned twin block ties are simpler, lighter, easier to handle, and less expensive and greater lateral resistance, and due to more flexible steel connections they are able to resist torsional force damage on the sleeper center. Bi-block sleepers are mostly used in ballastless track systems [38].

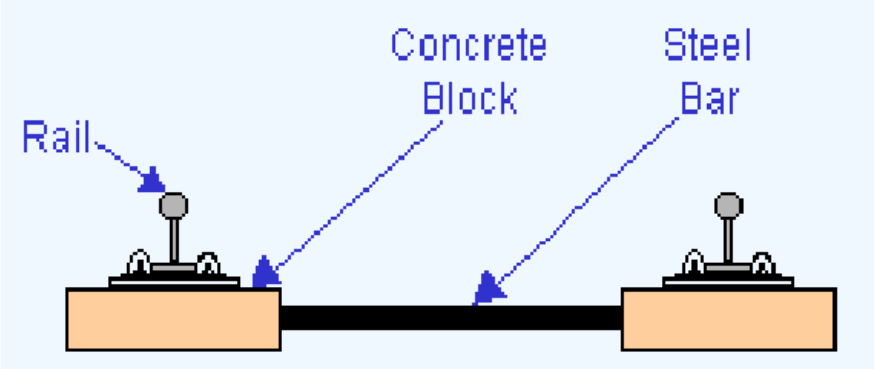

Figure 2.6 Two-block sleeper [37]

2.2.2 Limit States Concept

The objective of design is to obtain acceptable probabilities that a structure shouldn't become inadequate for its intended use, or that it will not reach a limit state. As a result, any circumstance in which a structure ceases to be fit for use will be considered a failure and the goal of the design is to prevent such a condition from occurring during the structure's expected life [39].

Limit state deems that the strength of a structure is satisfactory if its calculated nominal capacity, reduced by a capacity factor ϕ exceeds the sum of the nominal load effects multiplied by load factors**.**

$$\gamma \times Nominal\ load\ effects \leq \phi \times Nominal\ capacity$$

Where the nominal load effects (e.g. bending moments) are determined from the nominal applied loads by an appropriate method of structural analysis

Proposed limit states of pre-stressed concrete sleepers

Ultimate Limit State

A one-time event, such as a severe wheel, flat that generates an impulsive load capable of destroying a single concrete sleeper. Failure in such a severe event would fall under failure definitions that cause severe cracking at the rail seat or mid-span. [40].

Ultimate Moment Capacity:

A PSC section's ULS moment capacity is calculated under the premise that plane sections remain plane. This is similar to how ordinary reinforced concrete is approached. The strain in bonded pre-stress steel equals the strain caused by the initial pre-stress plus the change in strain in the concrete at the pre-stressing steel level [41]

The following diagram shows the strain diagram at three stages of loading:

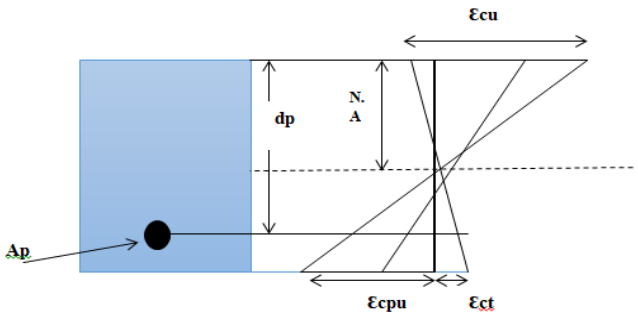

Figure 2.7 Strain diagram

Stage 1

This is the strain diagram at transfer. The strain in the concrete at steel is compressive, with magnitude of:

$$\varepsilon_{ct} = \frac{1}{E_c}\left(\frac{Pt}{Ap} + \frac{Pe^2}{I}\right) \qquad 2.3$$

Where

ε_{ct} is tensile strain for concrete

Pt is prestressing force

A is area of reinforcement bars

I Moment of inertia

The stress and strain in the pre-stressing steel are:

$$f_{pt} = \frac{P_t}{Ap} \qquad 2.4$$

Stage 2

The applied moment is sufficient to determine the concrete at the steel level. Provided there is a bond between the steel and concrete, the change in strain in the pre-stressing steel is equal to that of the concrete at the steel level. Hence the strain in the pre-stressing steel is now

$$\boldsymbol{\varepsilon_{pt} + \varepsilon_{ct}} \qquad 2.5$$

Where

ε_{ct} is tensile strain for concrete

Stage 3

This is the strain diagram at the ultimate load. The concrete strain at the steel level, ε_{cpu}, is related to the concrete strain at the top of the section by similar triangles)

$$\boldsymbol{\varepsilon_{cpu} = \varepsilon_{cu}\left(\frac{d_p - x}{x}\right)} \quad 2.6$$

Where ε_{cu} is ultimate compressive strain in the concrete

The change in strain in the pre-stressing steel is, by compatibility, the same as ε_{cpu}

Final

The final strain in the pre-stressing steel at ultimate load is thus:

$$\boldsymbol{\varepsilon_{pu} = \varepsilon_{pt} + \varepsilon_{ct} + \varepsilon_{cpu}} \quad 2.7$$

In this equation, it is only $\boldsymbol{\varepsilon_{cpu}}$ that is not known. This can be obtained once a depth of neutral axis is found that balance horizontal forces.

Proposed Ultimate Limit State Design Equations:

$$0.8Mu \geq M^* = 1.1M_Q + M_I \quad 2.8$$

Where

M_Q is the moment induced in the sleeper by the design value of the wagon weight force;

M_I is the moment induced in the sleeper by the ultimate impact force I for the specified return period;

M* is the bending moment at a cross-section calculated using the design load [34].

Fatigue Limit State

A time-dependent limit state in which a single concrete sleeper accumulates damage progressively over years until it is considered to have failed. Such failure could result from excessive accumulated

abrasion or from cracking that has become progressively more severe over its lifetime as a result of repeated loading impact forces [42].

Serviceability Limit State

This limit state denotes a situation in which sleeper failure is beginning to restrict the track's operating capability. A single sleeper failure is seldom the cause of a speed restriction or line closure. When a cluster of sleepers fails, however, an operational limitation is normally imposed before the issue is resolved [43].

2.2.3 Permissible Stress Principle

This is the most commonly used method for creating sleepers . The allowable stress theory, on the other hand, disregards the ultimate strength of materials, the probabilities of actual loads, and the possibility of failure, which may lead to the conclusion that current pre-stressed concrete sleepers are ineffective and overdesigned [44].

Table 2.1 Maximum permissible stress in the concrete at transfer[34]

Type of stresses	**Maximum Permissible stress**
Stress of Compression where the distribution of stress is triangular or approximately triangular	$\mathbf{0.6}f'_{cp}$
Compression where the distribution of stress is uniform or approximately uniform	$\mathbf{0.5}f'_{cp}$

Table 2.2 Maximum permissible stresses in the concrete, after allowing for all losses of pre- stress [34]

Type of stresses	**Maximum permissible stress**
compression	$\mathbf{0.4}f'_{c}$
Tension(flexure)	$\mathbf{0.4}(f'_{c})^{0.5}$

2.3 Failure modes of prestressed concrete sleepers

Critical performance criteria such as static capacity, dynamic strength and ultimate impact loading capacity should be evaluated as each property are mutually important and interconnected. Although the quasistatic capacity is often adopted in design process, the failure modes of the structural component must be known [31].

According to Remennikov, for static experiments, railway concrete sleepers appear to fail to bend or shear. In comparison, due to the splitting mode, the impact resistance of the railway concrete sleepers is most likely due to the splitting mode because of the shortage of bonding under complex conditions between pre-stressing wires and concrete [45].

Based on the research made by Jabbar-Ali, through manufacturing and maintenance, most defects occur after the operation stage. Among the statistical society surveyed, 1.2% of sleepers generated had defects, 0.3% of which are used in secondary lines and the remaining 0.9% are discarded [14].

Rail-seat deterioration and longitudinal cracking are the two key modes of concrete sleeper failure. A concrete sleeper's longitudinal cracking can be managed by introducing a special expansive concrete around the bolt-hole area while it can be put in transverse reinforcing bars, particularly around the bolt hole, to reinforce it transversely [46].

The results of North American and global surveys [25] have been received and ranked as the most common reasons for concrete sleeper failures as it is shown in table 2.3 . The end result has been specified that the primary cause of concrete sleeper failure is deterioration of rail seats in North America and the installation or tampering cause global harm However, this varies by country.

Table 2.3 Common damages of prestressed concrete sleepers.

Main causes	**Damages**	**North Ameri-can rank**	**International rank**
Lateral load	Abrasion of concrete material on rail seat	6.43	3.15
	Shoulder /fastening system wear or fatigue	6.38	5.5
Vertical dynamic load	Cracking from dynamic loads	4.83	5.21
	Derailment damage	4.57	4.57
	Cracking from center binding	4.5	5.36
Manufacturing and maintenance defects	Tamping damage (or impact forces)	4.14	6.14
	Other(e.g.: manufactured defect)	3.57	4.09
Environmental consid-erations	Cracking from environmental or chemical degradation	3.5	4.67

2.3.1 Rail-Seat Deterioration (RSD)

RSD is the deterioration of the concrete structure at the interface between the rail seat and the rail pad, and it can cause issues such as loss of cant, gauge-widening, fastener system wear, and other track geometry defects that create the potential for unstable rail conditions [47].

Based on RSAT (Rail Seat Abrasion Test) experiment made by Ryan G Kernes, et.al [47] , the research shows that abrasion is a feasible mechanism of RSD. Based on the results of the experiments, the frictional characteristics of the touch interface between the rail pad and the concrete rail seat tend to have an effect on the movement of forces and relative motion and thus on the process of abrasion.

The research from Office of Research [48], Development and Technology Washington, DC 20590, Results of the rail uplift test indicated that with increasing uniform RSD, both the gage and field side fastener toe loads were reduced. The key contributor to decreased rail longitudinal restraint is this reduction in toe load across the rail bench. With increasing uniform RSD, trials showed substantially less longitudinal rail restraint. Since the gage side, clip toe load is less affected in triangular RSD situations; longitudinal rail restriction has been less affected by increasing triangular RSD magnitudes

According to Russel Lutch ,et al. [49] the abrasion of the rail seat happens more often on curved track sections as well. It occurs as a result of uneven loading between the inner and outer rails, as well as additional lateral forces produced as the train navigates a curve, but it is not the primary cause of abrasion. The study has shown that hydraulic pressures inside the air voids of the cement paste have been discovered to be the cause of oxidation, resulting in a microscopic explosion.
It was shown in this study that railroads and manufacturers have worked to secure the concrete in the rail seat using abrasion resistant materials and repair procedures to prolong the life of the tie.

2.3.2 Longitudinal cracking

Longitudinal cracking occurred along the sleeper due to longitudinal axle and at a distance between roll-plaques, causing the sleeper muscle component to be ungreased, incorrect screw driving machine output, and incorrect concrete vibration within the shape, human faults such as incorrect roll-plaque placement, incorrect mixing of concrete constituent material [50].
According to Jesús Donaire-Ávil, et al [51] in their work, it was shown that the possible longitudinal cracking connecting dowels, found in some real railway pre-stressed precast sleepers even before being built, and temperature was considered as the key study factor. The findings show that some apparently not significant changes in the sleeper design and tightening system, particularly with regard to the dowels, can be critical and cause stresses that can be responsible for longitudinal cracking.

2.4 Analysis and Design of Pre-stressed Concrete Sleepers

The main considerations that contribute in the analysis and design of sleepers are the static and dynamic loads imposed on the rail seats and depend upon the type of track (straight or curved), its construction and standard of maintenance, the axle load and axle spacing, the running characteristics, speed and standard of maintenance.

The ballast reaction of sleeper is based on the shape of the standard of maintenance of vehicle and also is based on the shape of sleeper, its flexibility and spacing, the unit weight of the rail, the standard of maintenance of the track and ballast characteristics [34].

General condition for design of sleeper

Type and spacing

The sleepers shall be prestressed concrete sleepers intended for track designs using centre to centre of 500 mm to 750 mm of spacing and the depth and width of the sleeper may vary throughout its length. The minimum length of the sleeper shall be determined by the bond development requirements of the prestressing tendons ant the base width shall be then determined by allowable bearing pressure [52].

Clear tendon cover

Minimum clear concrete cover to tendons at the soffit of the sleeper shall be 35 mm. elsewhere, the minimum clear concrete cover to tendons generally shall be 25 mm with the exception that the tendon may be exposed at end faces [53] .

2.4.1 Rail seat Load

In order to build a sleeper, it is necessary to assess the loads that will be transferred to it. The required flexural capacity is calculated using the ballast support experienced during the sleeper's life and the applied rail seat loads.

The rail seat load, Q_o is dependent on a number of factors. These include the weight of the rail spacing of the sleepers, the stiffness of the sleeper, the track modulus per rail, the rail pad stiffness [54].

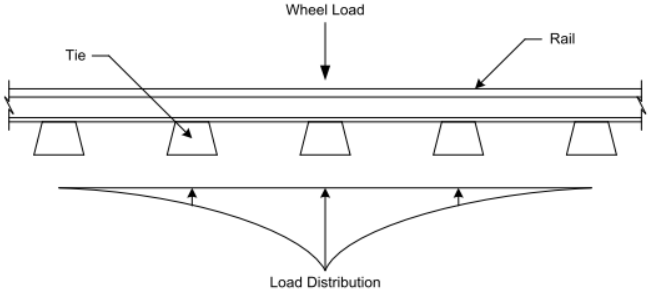

Figure 2.8 Distribution of load from single axle along track[55]

The load from an axle is spread among many links as a train travels along the track due to the track's rigidity. A single tie typically bears 45 to 55 % of the axle load immediately above it. The tie spacing, fastening system, rail stiffness, ballast and sub-grade conditions are all factors that influence load distribution, with tie spacing having the greatest impact [56].

2.4.2 Sleeper-ballast contact pressure

In the structural design of sleepers, the exact contact pressure distribution between the sleeper and the ballast, as well as its variance over time, will be important. Ballast support is critical to a tie's load-bearing capacity.

As a result, after applying wheel loads to the tie, wheel loads must be transferred to the ground through ballast and sub-ballast content. While an estimate is used to limit bearing pressures to avoid unnecessary track depression, the pressure between the tie and the ballast is not standardized across the bottom of the tie [57].

Ballast stiffness and yield ability are as follows: ballast stiffness is stress based, and repeated load applications result in greater deflection under rail seat than under center. It is possible that it'll end up with a center-bound track (this is similar to a uniform ballast pressure under load). As a consequence, broken connections can occur (at center) [58].

The ballast support forces changes as soon as the rail seat forces change. The configuration of ballast support forces is presented at lower as it is shown in figure 2.9 [59]

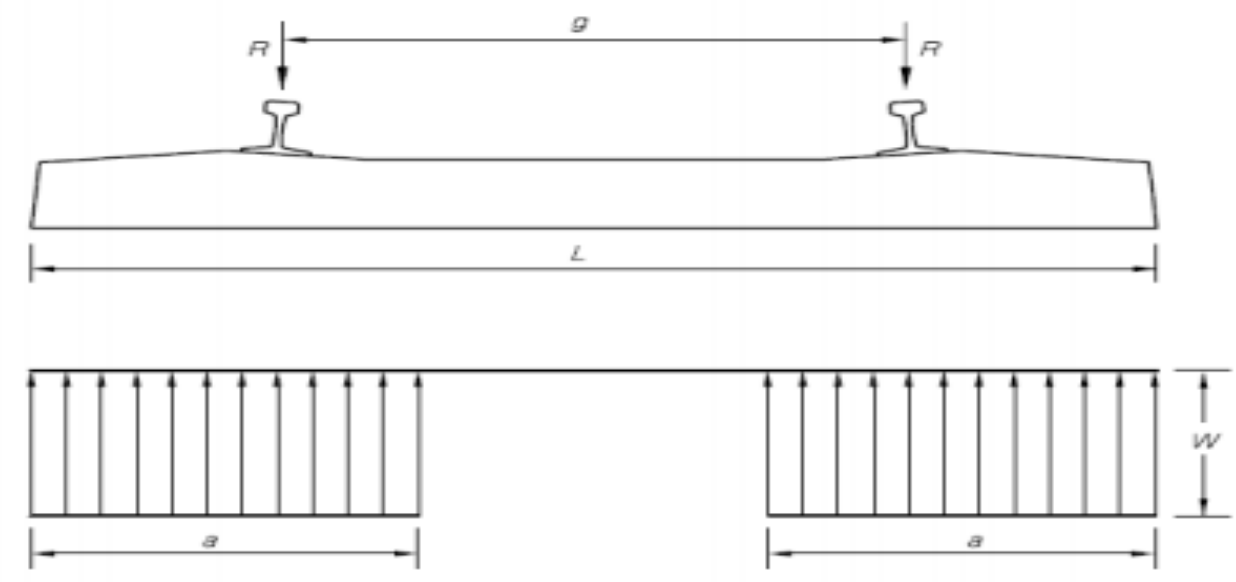

Figure 2.9 Force configuration of sleeper

2.5 Static behavior of prestressed concrete Sleepers

2.5.1 General Static Analysis

The overall static analysis can involve both linear and nonlinear effects and is conducted due to a static load, such as deflection, to determine static behavior. A condition for the analysis to be feasible is that it is stable. A static phase uses time intervals as a fraction of the load applied, not as dynamic measures [60]**.**

According to S. Kaewunruen [61], the rotational capacity, post-failure mechanisms, and residual load-carrying capacity of prestressed concrete sleepers under static loading were studied, and the static results were found to be in good agreement with the manufacturer's sampling tests. It is clear that the prestressed concrete sleeper has a low ductility. Furthermore, the modified compression field theory is found to be capable of predicting the static responses of prestressed concrete sleepers.

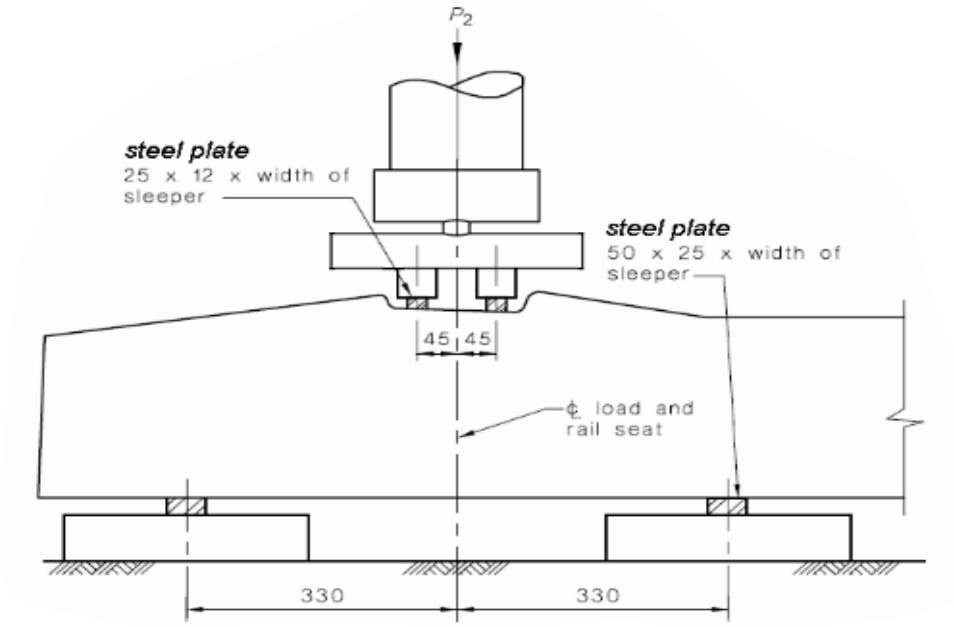

Figure 2.10 Schematics of a static test

Table 2.4 Experimental moment capacities of PCSs [61]

Loading	Target conditions	Tested moment at failure(kNm)	Type of damage
Static	crack	34	First crack is due to bending
	Fail	84	Shear failure
Dynamic	crack	44	First crack is due to bending
	Fail	95	Bending –shear failure

2.6 Mathematical model for Railway

The mathematical model for studying behavior of the track is categorized into three parts: beam on elastic foundation, vehicle track model, and discrete component models.

2.6.1 Beam elements

Beam elements have been used for the rails and sleepers modelling. A beam element is an element in which assumption are made so that the problems reduced to one dimension mathematically. The primary solution variable is then functions of the length direction of the beam. For this solution to be valid, the length of the element must be large compared to its cross-section. [60]

2.6.1.1 Beam on Continuous Elastic Support

The mathematical modeling is done on the elastic foundation of the Winkler type, with the railway track acting as an Euler Bernoulli beam. According to Winkler, when a beam rests on an elastic foundation under the action of an externally applied load, the reaction forces of the foundation are proportional to the deflection of the beam at every point [62].

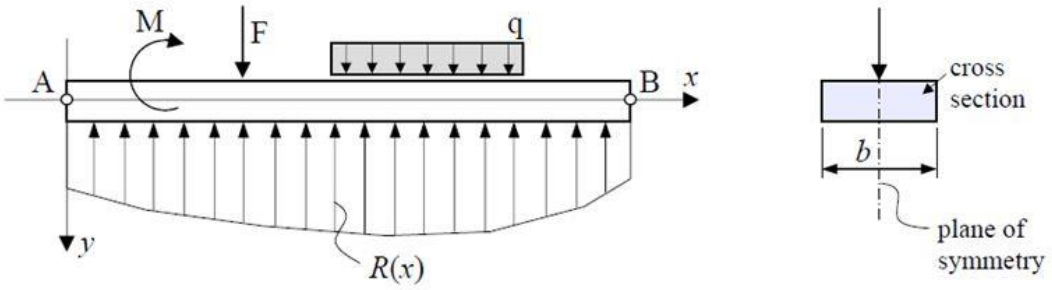

Figure 2.11 Beam (bending stiffness EI) on elastic foundation

The model has a strong mathematical formulation with a plain and simple physical formulation. It assumes that the rail is built as an infinite beam of Euler-Bernoulli

The general 4 th order differential equation for a beam on an elastic foundation is given by the equation below:

$$EI\frac{d^4y}{dx^4} + ky = q \qquad 2.9$$

Where:
x = the length coordinate
q = the distributed load on the rail
EI = the beam bending stiffness EI (Nm)
k = the foundation stiffness (N/m per m)

The homogeneous equation is given by

$$EI\frac{d^4y}{dx^4} + ky = 0 \qquad 2.10$$

$$EI\frac{d^4y}{dx^4} + 4\beta^4 y = 0 \qquad 2.11$$

By introducing a parameter β (unit L^{-1})

$$\beta = \left(\frac{k}{4EI}\right)^{1/4} \qquad 2.12$$

The solution of the governing equation can be written as

$$y = e^{\beta x}(C_1 \sin\beta x + C_2 \cos\beta x) + e^{-\beta x}(C_3 \sin\beta x + C_4 \cos\beta x) \qquad 2.13$$

Where the constants C_1, C_2, C_3 and C_4 are computed with following formula as it is shown from Roark 'formulas for stress and strains[63]

$$C_1 = cosh\beta l cos\beta l \qquad 2.14$$

$$C_2 = coshβlsinβl + sinhβlcosβl \quad 2.15$$

$$C_3 = sinhβlsinβl \quad 2.19$$

$$C_4 = coshβlsinβl - sinhβlcosβl \quad 2.20$$

2.6.2 Elastic foundation models

The computational model of a structure on an elastic foundation is frequently used to describe a wide range of engineering problems, with applications in geotechnics, road, railroad, and marine engineering, as well as biomechanics. Modeling the interaction between the structural elements the sleeper and the ballast is the most important aspect of the analysis.

2.6.2.1 Ballast Support

The railway ballast layer, as an important component of the railway track system, must achieve the following important goals: stress transfer, high resistance to longitudinal and lateral displacement of sleepers, increased elasticity, increased longitudinal and lateral stability of railway tracks, and easy repair and maintenance of railway track[64]

In actual fact, the pressure between the sleeper and the ballast is not uniform across the bottom of the sleeper. So, an approximation is used to limit bearing pressures and prevent excessive track depression. According to AREMA section 4.1.2.5, the average ballast pressure is a function of the applied axle loads, impact factors, and tie bearing area. It is essential that the ballast and sub-ballast are not over stressed to prevent accelerated deterioration to the track and the ballast itself due to excessive depression of the track [65]

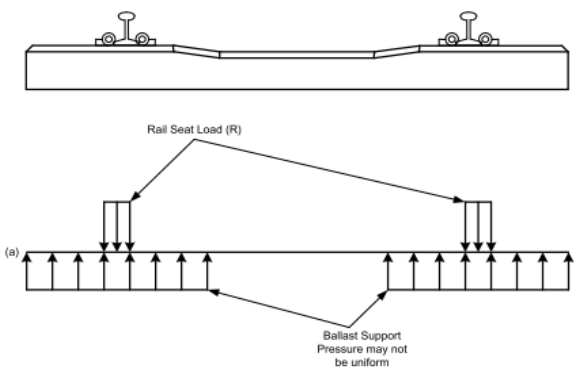

Figure 2.12 Ballast pressure distribution

2.7 Concrete sleeper modeling

In various researches the most popular finite element packages like Abaqus, Ansyss, and LS-DYNA have been used for numerical modeling.

Remennikov and Kaewunruen [66] did their work by modeling a prestressed concrete sleepers with holes and web opening and Abaqus was used for determining structural capacity and toughness of prestressed concrete with and without holes. It was found that the results from finite element modeling have been validated using experimental works where there was a good correlation between the results from model and experiment.

Another research entitled “Experimental and Numerical Studies of Railway Prestressed Concrete Sleepers under static and impact loads” was also done by Remennikov and Kaewunruen where a three-dimensional non-linear finite element model of a railway prestressed concrete sleeper was developed using the general purpose finite element analysis package, ANSYS10 and LS-Dyna [67] .

In this study ABAQUS was used for numerical analysis of prestressed concrete sleepers under static loads where elastic foundation was considered as support condition.

Chapter 3: MATERIALS AND METHODS

3.1 Prestressed concrete sleeper Analysis and Design.

The load distribution beneath the sleeper and its variation over time has a significant impact on the structural design of the sleepers.

3.1.1 Flexural capacity of sleeper

The rail seat and ballast pressure loads determine the flexural capacity of the sleeper. According to AREMA 2010, the positive and negative moments are located at the rail seat and in the sleeper's center [34].

The structural design process for prestressed concrete sleepers consists of two steps. First, an analysis is performed to estimate the demand (flexure, shear.) that a structural element is expected to undergo in its lifetime. Second, the element is designed to meet or exceed the demand found in the analysis[44].

Based on the elastic foundation beam model, the American Railroad Engineering Association (AREA) design method was developed to calculate the required minimum flexural capacity of sleeper in order to determine the maximum rail seat load. This method assumes a uniform distribution of contact pressure between sleepers and ballast, resulting in positive flexure at the rail seat and negative flexure in the middle of the sleeper.

The current AREMA method for concrete sleeper flexural analysis is a factored approach that is dependent on sleeper length, sleeper spacing, annual tonnage, and train speed. Design bending moments are given for four key locations on the sleeper: rail seat positive (MRS+), rail seat negative (MRS-), center positive (MC+), and center negative (MC-)

The forces acting on the underside of the rail and the seating area of the sleeper is called Rail Seat Load When designing sleepers, the ballast pressure should not exceed some limit (0.5 MPa according to BS)

The effective support area for sleepers

The product of the sleeper's width and the assumed value of the effective length of sleeper support at the rail seat yields the efficient sleeper support area beneath the rail seat. AREA defines the effective length of a sleeper as the distance from the end of the sleeper to the extent of tamping inside the rail foot.

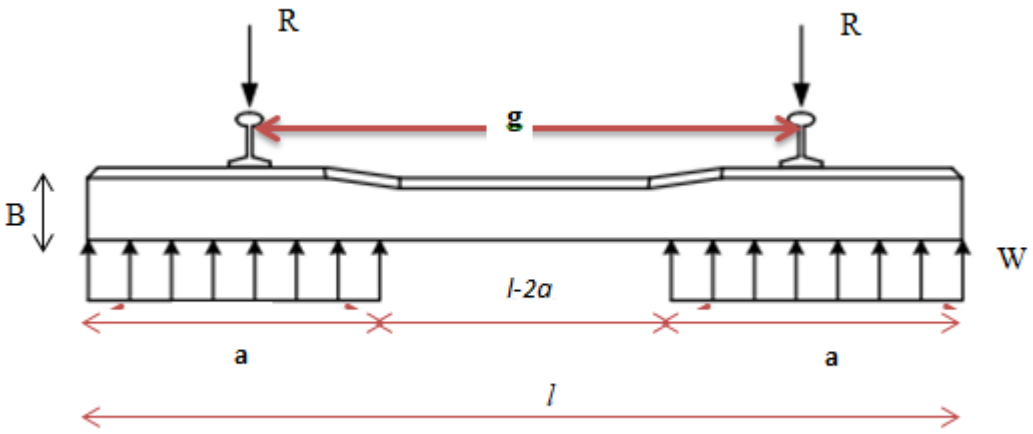

.

l = Total sleeper length (mm)

For wooden, steel, and concrete sleepers, Schramm describes the effective length of sleeper support under the rail seat as:

$$L = \frac{l - g}{2} \qquad 3.1$$

Table 3.1 The effective support area for sleepers[34]

Suggestion by:	**Effective length of sleeper support at the rail seat**
AREA	Distance from the end of the sleeper to the point inside of the edge of the the rail base over which tamping operations extend
Clarke	$L = (l - g)(1 - \frac{(l-g)}{125t^{0.75}})$ in which l, g and t are total sleeper length(mm), distance between the center- line of rail seats (mm) and sleeper thickness (mm) respectively
Schramm	$L = \frac{l - g}{2}$
Simplified Clarke	$L = \frac{l}{3}$

During Sleeper Analysis and design different important parameters should be considered which are the rail seat loading at the sleeper, effective bearing area of the sleeper and the flexural characteristics of the sleeper

Load distribution on the ballast

In the structural design of sleepers, the specific contact pressure distribution between the sleeper and the ballast, as well as its variation over time, will be critical. In the in-track condition, it's nearly hard to forecast the approximate distribution of a sleeper [58].

Load case 1: Over time settlement and ballast degradation lead to uniform ballast support inducing negative moment at center section and continued positive moment at railseat

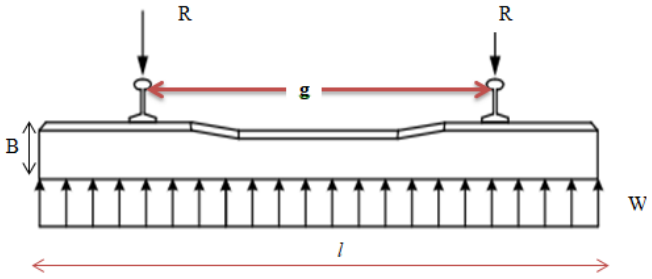

Load Case 2: After installation and tamping, ballast support limited to rail seat region producing positive moment in rail seat section

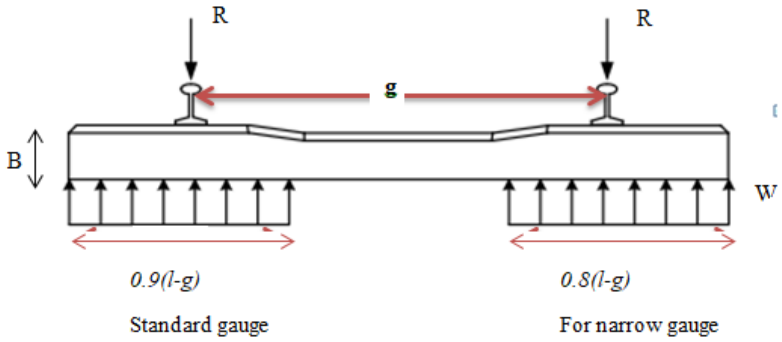

Figure 3.1 Pressure distribution for maximum centre moment positive

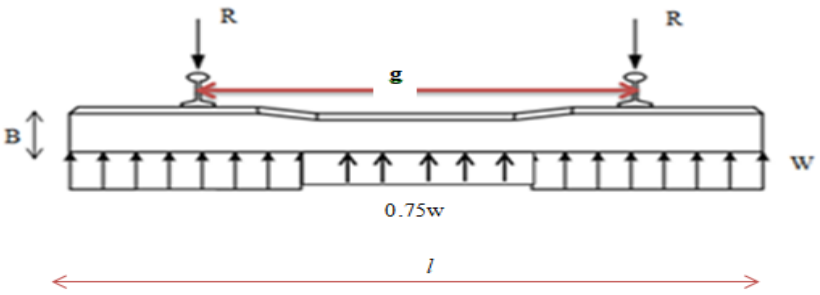

Figure 3.2 Pressure distribution for maximum centre moment negative

Bending moment in concrete sleeper

Bending moment distribution is related to the support condition of the ballast

Moment at the rail seat

1. Rail Seat Positive Design Bending Moment

The maximum positive bending moment shall be taken to occur at the rail seat producing compressive stress at the top and tensile stress at the underside of the sleeper. The value of this moment, the rail seat positive design bending moment (MR+), is based on a uniform ballast support beneath each rail seat.

The maximum positive sleeper bending moment at the rail seat *Mr* (KN m) is given by

$$M_r = \frac{w \times (l - g)^2}{8} \qquad 3.2$$

Where
l = total sleeper length (m),
g = distance between rail centres (m),
w = assumed uniformly distributed load (kN / m).

2. Center Negative design bending moment

The maximum negative sleeper bending moment at the centre of the sleeper *Mc* (KN m) is given by

$$M_C = \frac{R \times (2g - l)}{4} \qquad 3.3$$

Where
l = total sleeper length (m), g = distance between rail centres (m), R = Rail seat load

Table 3.2 Design pressures and moments-Empirical method [58]

Distance between rail centres(g)m	**Length of ballast support beneath each rail seat (a) m**	**Design values kPa or kNm**	
g> 1.5 m (standard gauge)	a =L-g	Design ballast pressure(P_{ab})	$Pab = \frac{R}{(w(L-g)}$
		Design Positive bending moment at rail seat(M_{R+})	$M_{R+} = \frac{R(L-g)}{8}$
		Design bending moment at rail seat(M_{R-}	$M_{R-} = 0.67M_{R+}$
	$a = 0.9(L-g)$	Design positive bending moment at the center(MC+)	$M_{C-} = 0.05\,R(L-g)$

Static Load

The load that comes from weight of train is considered as static load over the railway track. The value of static load related parameters are taken from ERC feasibility study and previous studies as shown Table 3.3 [35].

Table 3.3 Statistical parameters of static load

Parameters	**Unit**	**Value**	**Source**
Axle Load	kN	250	ERC feasibility study
Distribution factor	%	0.52	AS 1085.14 2003
Wheel Load	kN	125	50% 0f Axle load
Rail-seat load	kN	81.25	50%

Rail Seat Load

The rail seat load on individual sleeper is dependent on tie spacing, fastening system, rail stiffness, and ballast and sub-grade conditions with tie spacing having the largest effect. Typical track design with concrete ties utilizes tie spacing of 60cm which correlates with 50 percent of the applied axle load being carried by an individual tie.

The design static wheel load is the maximum load that can be applied to a wheel, as determined by the owner based on the tonnage and passenger weight of a vehicle with an axel load of 25 tons. According to Australian Standard vertical design load factor is 250 percent of the static load [68].

According to AS 1085.14 [68] the rail seat load (R) is given by:

$$R = \frac{Q}{2} \times DF \times \frac{I}{100} \qquad 3.4$$

Where

R = Rail seat Load

Q = wheel Load

DF= Distribution Factor

I =Impact Factor

The impact factor including all quasi-static factors said to be 250%

Therefore, the assumed uniformly distributed load **w (kN/m)** over the entire sleeper length *l(m)*

$$w = \frac{2R}{l} \qquad 3.5$$

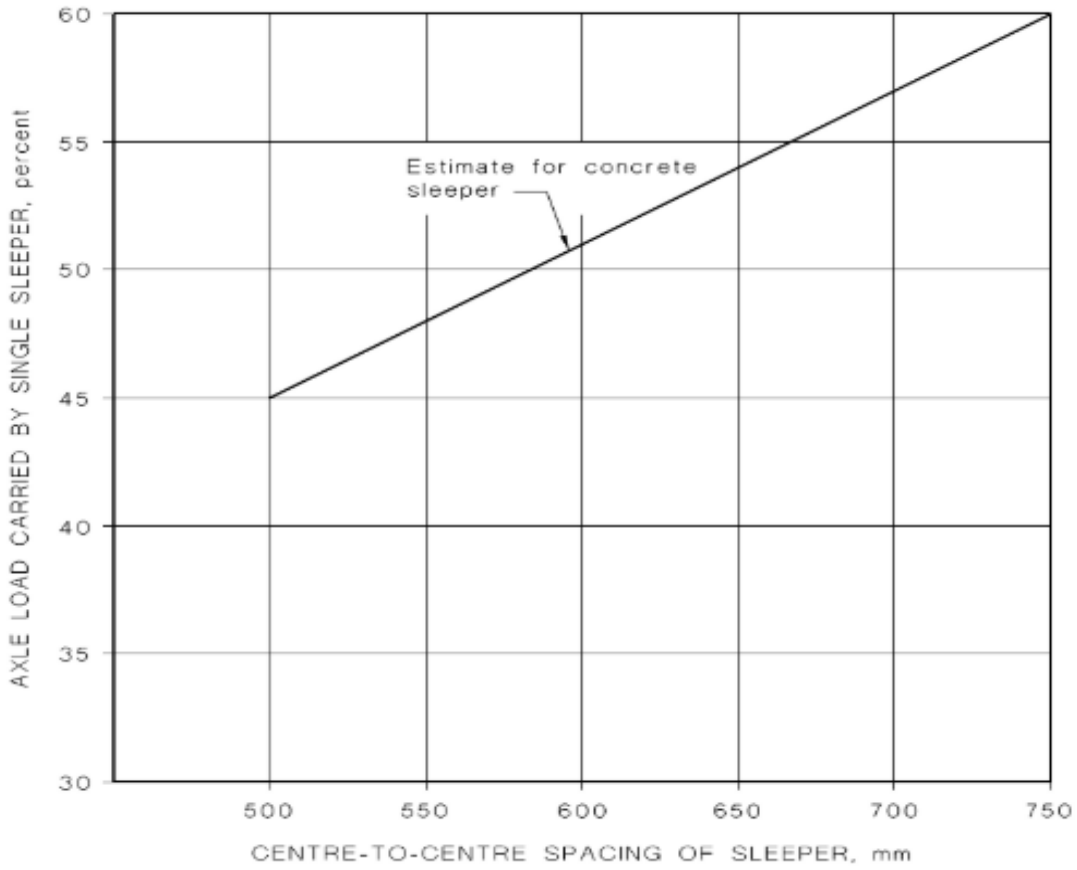

Figure 3.3 Estimated distribution of load (D.F), AS 1085.14-2003

3.3 Finite Element Modeling

To investigate the performance of concrete sleeper (such as deformations and Stresses), a finite element model was developed using ABAQUS software package under Static loading

3.3.1 Validation of the FEM

In this section of a finite element model (FEM) validation for sleeper, the model is established Using Finite Element package – Abaqus, which is a numerical tool used to model and simulate the mechanics behavior and response of sleeper. In this study, only static structural analysis was conducted. The following sections outline the properties of concrete and prestressing steel wires used as input values in finite element analysis.

3.3.1.1 Material properties

Concrete material

The railway sleeper is made of concrete material. The typical properties of normal strength Concrete C55/67 used as input data:

Density (Kg/m^3)	Young's Modulus (MPa)	Poisson's ratio	Compressive strength (MPa)	Tensile strength (MPa)
2400	30200	0.2	55	2.85

In order to capture crushing and cracking of sleepers, non-linear elastoplastic behavior of concrete is assumed when modeling. As a result, the following is a list of plastic behavior:

Plastic stress-strain relation for concrete

Yield stress (MPa)	Plastic strain
30	0
50	0.001
48	0.003

Pre-stressing reinforcement material

Prestressed reinforcement in sleeper that can increase tensile capacity of the sleeper is also of importance.

Typical properties of reinforcement are indicated below:

- Density: ρ = 7.8 g / cm^3
- Young's modulus: E = 200 GPa
- Poisson's ratio: v= 0.3
- Thermal expansion: a = 1.1 * e-5

Plastic stress-strain relation for steel material is shown below

Yield stress (MPa)	**Plastic strain**
0.01	0
1703	0.0085
1750	0.0097
1797	0.01
1978	0.064

3.3.2 Static Modeling of Sleeper with Fixed Support

Model components dimensions

Front view of the sleeper

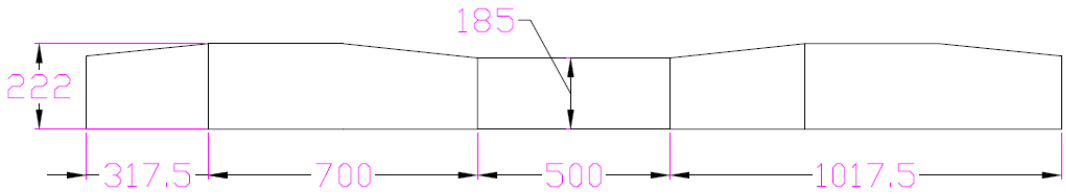

Top view of the sleeper

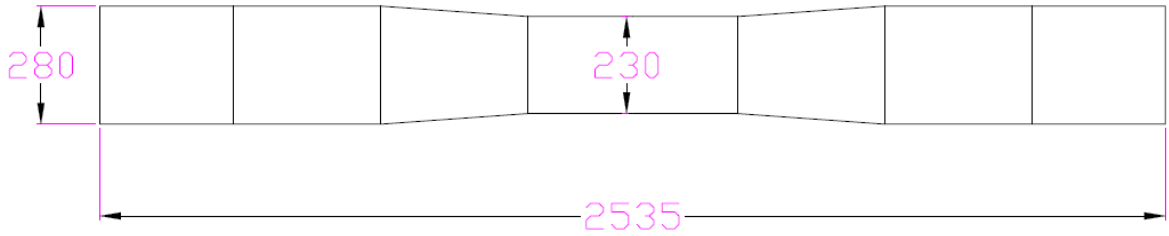

Side view of the sleeper The transparent part showing inside bars

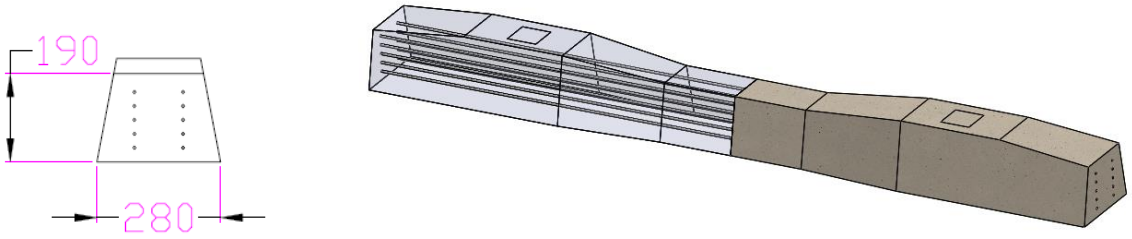

Figure 3.4 Skectch of modeled prestressed concrete sleeper

Three-dimensional elements have been used to model pre-stressed concrete sleeper and reinforcement bar elements. This model can help to confirm the theoretical calculations as well as to provide a valuable supplement to the experimental investigations of behavior of pre-stressed concrete sleepers

Element selection

Because the purpose and desired output vary from model to model, a variety of element types exist for both steel and concrete materials. The elements used in modeling prestressed concrete sleepers are summarized below.

Solid Elements

The concrete section is represented by a three-dimensional solid element, SOLID65, which includes a material model for predicting brittle element failure. This element has eight nodes, each with three degrees of freedom in the nodal x, y, and z directions. Because of built-in algorithms that are dependent on the SOLID65, it is capable of cracking tension and crushing in compression[34]

As the force / moment redistribution, the concrete sleeper is currently designed to resist prestressing force completely throughout the entire cross-section. As a result, the smeared crack cannot be used to replace prestressing tendons in fully prestressed structures [69][69].

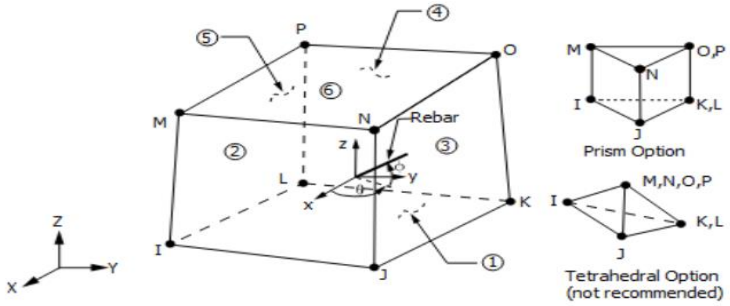

Figure 3.5 SOLID65 Element

Bar Elements

The ability to perform inelastic behavior and define an initial strain are two necessary element characteristics for modeling pre-stressing. It is recommended starting with the LINK8 element in order to withstand the initial strain attributed to prestressing forces, as a typical truss element cannot resist neither bending moments nor shear forces

An advantage of the LINK8 element is the ability to specify an initial strain. This is useful for defining the initial pre-stressing force. In addition, pre- stressing transfer can be completed by simply varying the initial strain along the length of the steel mesh.

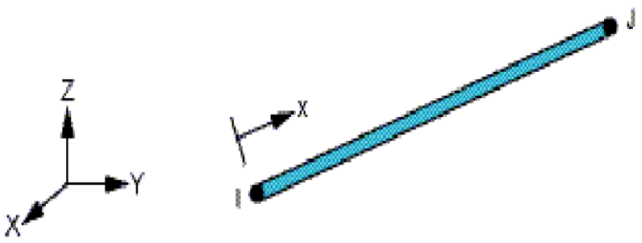

Figure 3.6 LINK8 elements

With the experiment performed by Rikard [71], a simple static sleeper model with fixed support condition is modelled, analyzed, and the obtained results are compared to the experiment performed by Rikard in order to assess the quality of the FE model and validate it in comparison to existing ones. Six Abetong Teknik AB type A9P sleepers were cut in the middle perpendicular to the sleeper line.

Each half-sleeper was bent to produce the same primary deflections as if it were in a track system. The static study is performed out using a hydraulic jack. A load ranging from 0 to 237.5 KN is applied to the rail seat area. In this case, the support condition is fixed where sleeper is tied on the ground on four locations as shown in figure 3.8

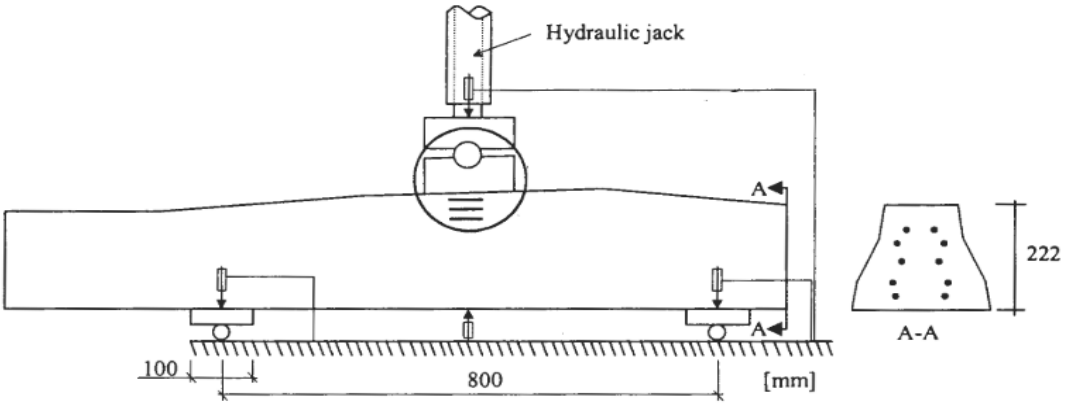

Figure 3.7 Test set-up used in the test done by Rikard [70].

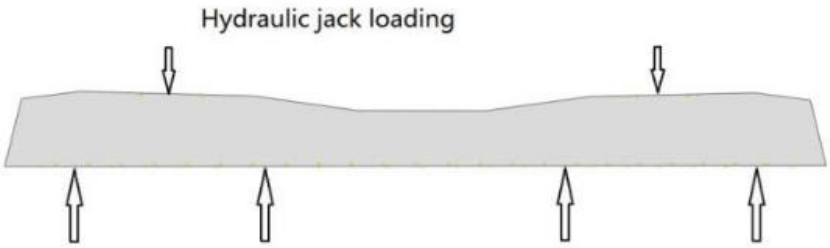

Figure 3.8 Static structural model with fixed support [69]

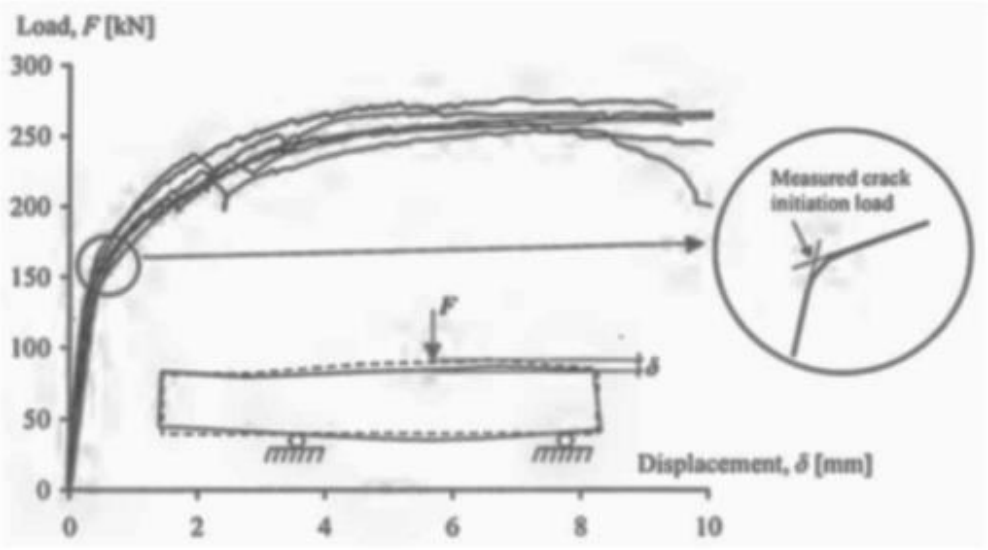

Figure 3.9 The load-vertical displacement relation for the six tested half-sleeper

Numerical results

To validate the effectiveness of this FE model, the sleeper was subjected to the same hydraulic jack loading as Rikard and the load applied to the rail seat area is varying from 0 to 237.5 KN. The model was then meshed with size of 25 mm as shown in figure 3.11 and its computational results are then compared to those of Rikard [70], using the load-defection graph.

Static modeling of sleeper type A9P

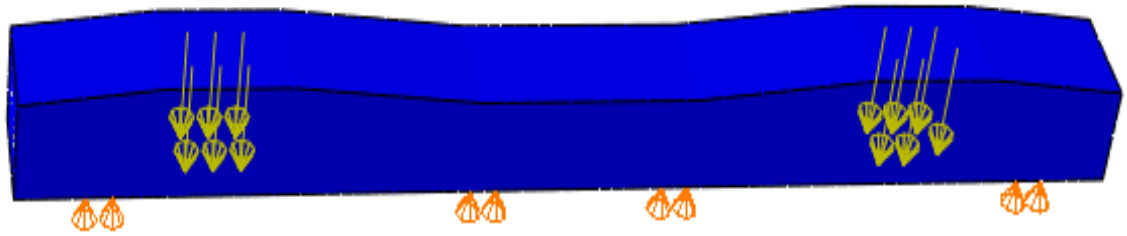

Figure 3.10 Prestressed Concrete sleeper with applied load

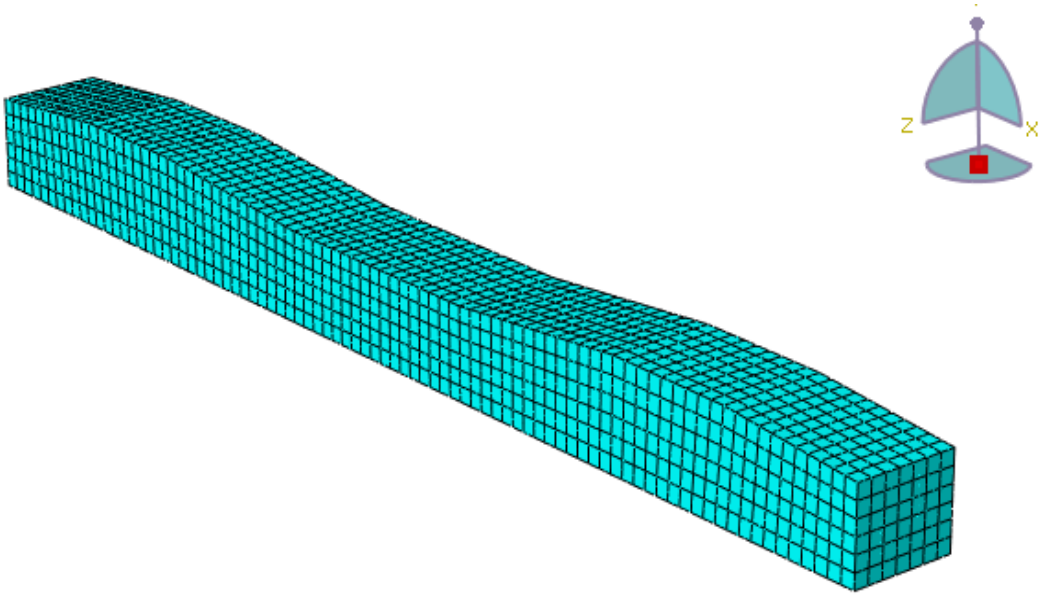

Figure 3.11 Meshed sleeper model

FEM results

Load (kN)	Deflection(mm)
0	0
50	0.2535
150	1.065
200	1.782
237.5	3.779

Experiment results

Load(kN)	Deflection(mm)
0	0
50	0.25
150	1
200	1.875
237.5	4

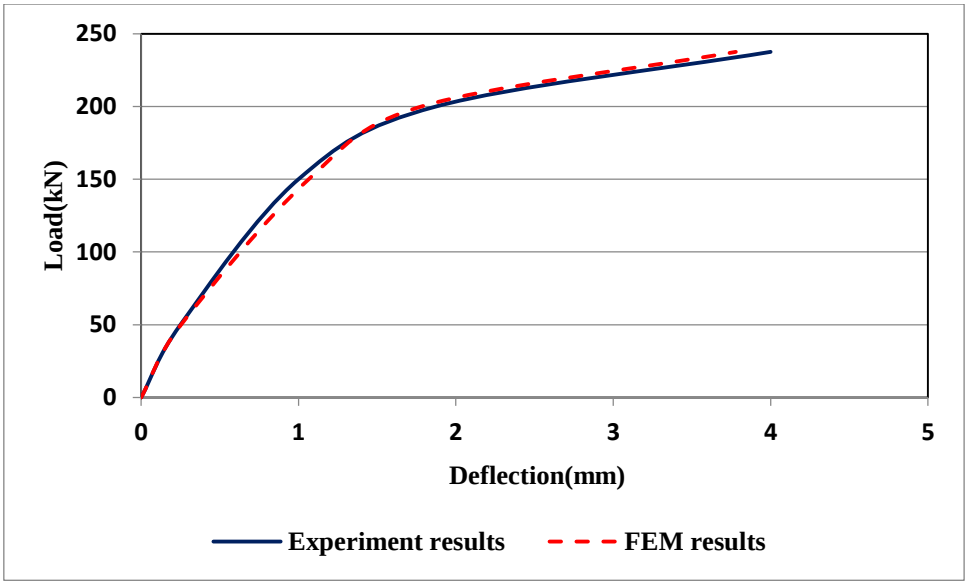

Figure 3.12 Load –deflection graph with FEM results and experimental results

As demonstrated in Figure 3.12 the force and deflection diagrams match Rikard[70], indicating that the FE model is of acceptable quality. After the model has been validated in relation to the test findings, the FE-model can be used for further investigation. Therefore, as the static results match the experimental results; static simulations can be performed using ABAQUS software.

3.4 Static modeling

The total length of sleeper is 2.5 m. The central distance between the rail seats (standard gauge distance) is 1.435 m.

Loading conditions

The effective sleeper support area

The useful sleeper support area beneath the rail seat is calculated as the product of the sleeper's width and the assumed value of the effective length of sleeper support at the rail seat. The effective length of a sleeper is defined by AREA as the distance from the end of the sleeper to the extent of tamping inside the rail foot.

In this thesis**,** the effective length used is $\boldsymbol{L = l/3}$

Where L = Effective length of sleeper support (mm) and l = Total sleeper length (mm) g is the distance between the center lines of the rail seats in mm

Rail seat load

In this study, the value of 0.52 was used as per figure 3.3 for a sleeper spacing of 60 cm.

Therefore, the rail seat load was computed as from equation 3.4

$$\boldsymbol{R = \frac{250}{2} \times 0.52 \times \frac{250}{100} = 162.5kN}$$

Table 3.4 Material properties [34]

NO	**PROPERTIES**	**VALUE**
	CONCRETE	
1	Density(ρs)	2400kg/m^3
2	Young Modulus(Ec)	37000 MPa
3	Poisson's ratio(υc)	0.2
4	Thermal expansion(αc)	1e-5
5	Strain value	0.0035
6	Compressive strength	55MPa
7	Tensile strength	2.97 MPa
	PRESTRESSING WIRES	
1	Density(ρs)	7800kg/m3
2	Young Modulus(Ec)	200,000MPa
3	Poisson's ratio(υc)	0.3
4	Characteristic strength	1570MPa
5	Strain value	0.00542
6	Yield strength	1770MPa
7	Tensile strength	1085MPa

Table 3.5 Maximum permissible stresses in concrete under working conditions as per AREMA

Types of stress	**Maximum permissible stress**
compression	0.45*fc'
Tension	$0.62(fc')^{0.5}$
fc' is the concrete strength	

The controlled stress for stretching prestressed reinforcement must not exceed the allowable controlled stress for stretching as specified in table 3.6 and must not be less than $0.4*f_{plk}$

The standard further recommends an intended stress-relieved prestressing steel wire of diameter of 5 or7mm, in this study 10 prestressing steel wires of diameter of 7mm were used and elastic foundations was considered as support conditions.

In this model, one monoblock prestressed concrete sleeper was studied by considering 3 equal parts along the total distance of the sleeper, and each part has its corresponding ballast stiffness that are K_1,K_2 and K_3, which are at the rail seat, the centre of the sleeper.

Where *Ks* = ballast stiffness per sleeper and equals to 250 MN /m [71].

$$K_i = a_i \times K_s \quad i = 1,2,3$$
$$K_1 = a_1 \times K_s$$
$$K_2 = a_2 \times K_s$$
$$K_3 = a_3 \times K_s$$

Where

a_1, a_2, a_3 are distribution coefficient

K_1 is base support stiffness for first part of the sleeper (under rail seat)

K_2 is base support stiffness for second part of the sleeper (center of the sleeper)

K_3 is base support stiffness for third of the sleeper (under rail seat)

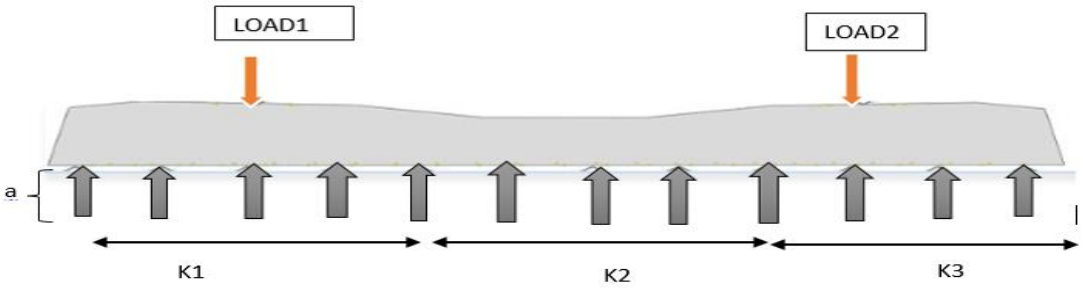

- After modeling the results like displacement and stresses have been highlighted
- Different curves and graphs have been displaced to show the displacement and stresses under different elastic foundation using different distribution coefficients
- Incremental percentage for displacement and stresses was computed using the following formal

$$I(\%) = \frac{(FS\ displacement - PSdisplacement) \times 100}{FS\ displacement} \qquad 3.6$$

$$I\% = \frac{(FS\ stress - PS\ stress) \times 100}{FS\ stress} \qquad 3.7$$

Where

I(%)=Incremental percentage, FS= Full Supported, PS= Partially supported

- First modeling: Ballast stiffness reduction at the center of the sleeper

Case	a_1	a_2	a_3	K_1(MN/m)	K_2(MN/M)	K_3(MN/m)
1	1	1	1	250	250	250
2	1	0.9	1	250	225	250
3	1	0.8	1	250	200	250
4	1	0.7	1	250	175	250
5	1	0.6	1	250	150	250
6	1	0.5	1	250	125	250
7	1	0.4	1	250	100	250
8	1	0.3	1	250	75	250
9	1	0.2	1	250	50	250
10	1	0.1	1	250	25	250

- Second modeling: Uniformly ballast stiffness reduction along the sleeper

Case	a_1	a_2	a_3	K_1(MN/m)	K_2(MN/M)	K_3(MN/m)
1	1	1	1	250	250	250
2	0.9	0.9	0.9	225	225	225
3	0.8	0.8	0.8	200	200	200
4	0.7	0.7	0.7	175	175	175
5	0.6	0.6	0.6	150	150	150
6	0.5	0.5	0.5	125	125	125
7	0.25	0.25	0.25	62.5	62.5	62.5

Chapter 4: ANALYSIS RESULTS AND DISCUSSION

4.1 Design of prestressed concrete sleeper

Flexure Strength of Prestressed concrete sleeper

Table 4.1 Dimensions of the sleeper

Sleeper length (L)	2500 mm
Rail seat width (Top)	170 mm
Rail seat width(bottom)	280 mm
Center width(Top)	200mm
Center width(Bottom)	250mm
Height rail seat	200mm
Height of sleeper centre	160 mm

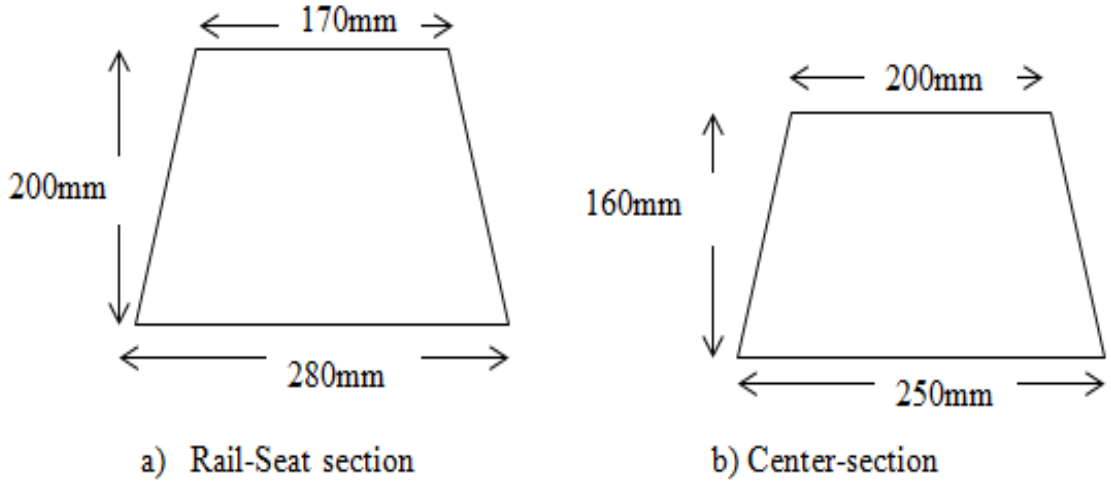

Figure 4.1 Cross-section of the sleeper

1. At Rail seat:

- Area calculation (A_r)

$$A_r = \frac{(280 + 170) \times 200}{2} = 45000mm^2$$

- Center of gravity from bottom (Yb)

$$Y_b = \frac{(2 \times 170 + 280)}{170 + 280} \times \frac{200}{3} = 91.85mm$$

- Center of gravity from top (Y_t)

$$Y_t = \frac{(2 \times 280 + 170)}{280 + 170} \times \frac{200}{3} = 108.15mm$$

- Moment of Inertia($_{Ir}$)

\

$$I_r = \frac{\frac{(200^3(170^2 + 280^2 + (4 \times 170 \times 280)}{36}}{170 + 280} = 147 \times 10^4 mm^4$$

- Section modulus from bottom (Zb)

$$Z_b = \frac{147 \times 10^4}{91.85} = 1.6 \times 10^4 mm^3$$

- Section modulus from top(Zt)

$$Z_t = \frac{147 \times 10^4}{108.15} = 1.36 \times 10^4 mm^3$$

2. at center of the sleeper

- Area calculation (Ac)

$$A_c = \frac{(250 + 200) \times 160}{2} = 36000mm^2$$

- Center of gravity from bottom (Yb)

$$Y_b = \frac{(2 \times 200 + 250)}{200 + 250} \times \frac{160}{3} = 77.03mm$$

- Center of gravity from top (Yt)

$$Y_t = \frac{(2 \times 250 + 200)}{250 + 200} \times \frac{160}{3} = 82.96mm$$

- Moment of Inertia(Ic)

$$I_c = \frac{\frac{(160^3(200^2 + 250^2 + (4 \times 200 \times 250)}{36}}{200 + 250} = 76.48 \times 10^6 mm^4$$

- Section modulus from bottom (Zb)

$$Z_b = \frac{76.48 \times 10^6}{77.03} = 0.99 \times 10^6 mm^3$$

- Section modulus from top(Zt)

$$Z_t = \frac{76.48 \times 10^6}{82.96} = 0.92 \times 10^6 mm^3$$

4.1.1 Prestressing force calculation

The concrete around the tendons shortens as the prestressing force is applied. The concrete surrounding the tendon is shrinking, causing the tendon to lose stress. It is proportional to the amount of shrinkage that occurs after prestress force is applied to concrete.

$$P_t = f_{ct} \times A_c \leq 0.75 f_{pt} \times A_p \qquad 4.1$$

Where, P_t is allowable prestress force, f_{ct} is allowable stress of concrete under compression
A_c is net area of concrete

The area of concrete can be considered to be equal to the gross size of the section for preliminary parameter iteration. However, the concrete cross-section is divided into two parts for final design: the net area of the concrete section (A_c) and the area of prestressing steel (A_p)

$$A_g = A_c + A_p \qquad 4.2$$

For preliminary design, 10 bars of diameter of 7mm is used

$$A_P = 10 \times \frac{22 \times 7^2}{7 \times 4} = 385 mm^2$$

Using the average width and height of the sleeper the net area of concrete was computed in order to estimate prestress force at transfer after short-term loss.

$$A_g = 165 \times 270 = 44550 mm^2$$

$$A_C = A_g - A_p = 44550 - 385 = 44165 mm^2$$

The prestressing force at transfer is calculated with equation 4.1

$P_t = 22.68 \times 44165 = 100166N > 0.75 \times 1860 \times 385 = 537\,075\ N$ not ok!

Let use $P_t = 537\,075\ N$

4.1.1.1 Compression Force of Concrete

The real distribution of compressive stress in a prestressed concrete part indicates rising parabola shape. If the compressive stress block has a parabolic shape, determining its volume takes time. To calculate the compressive force in this investigation, an equivalent rectangular stress block was employed instead of the ascending parabola. This corresponding stress block comprises a depth and an average compressive strength of ηf_{cd}.

All dimensions are in mm

A) Rail Seat

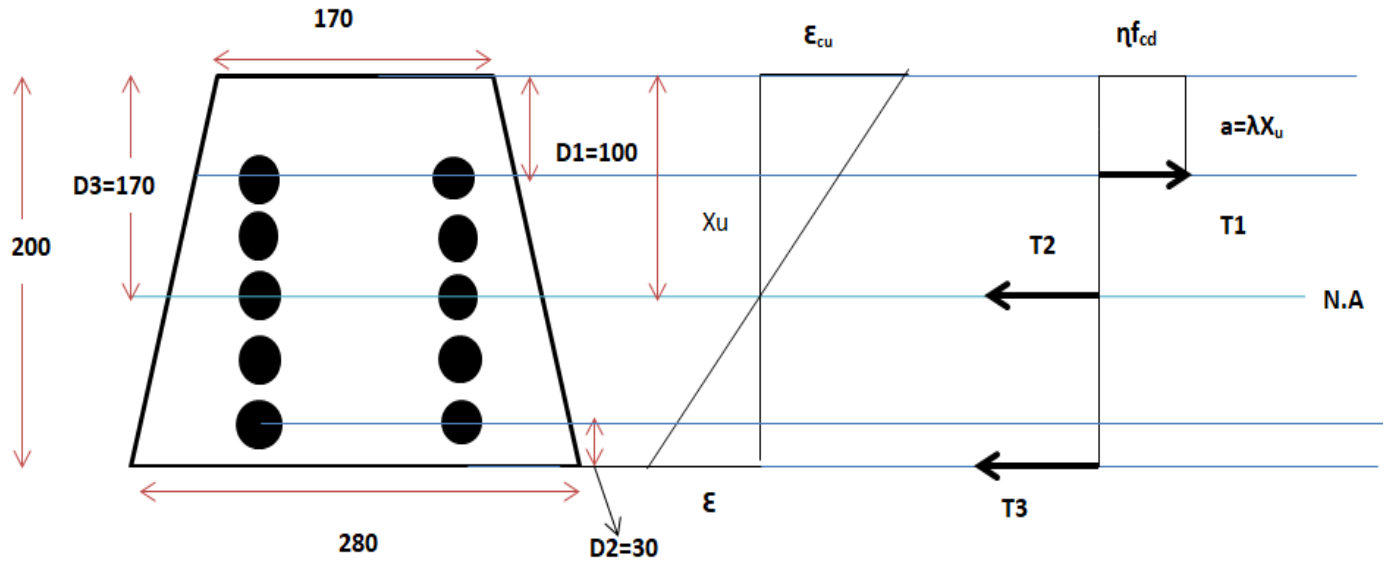

B) Center of sleeper

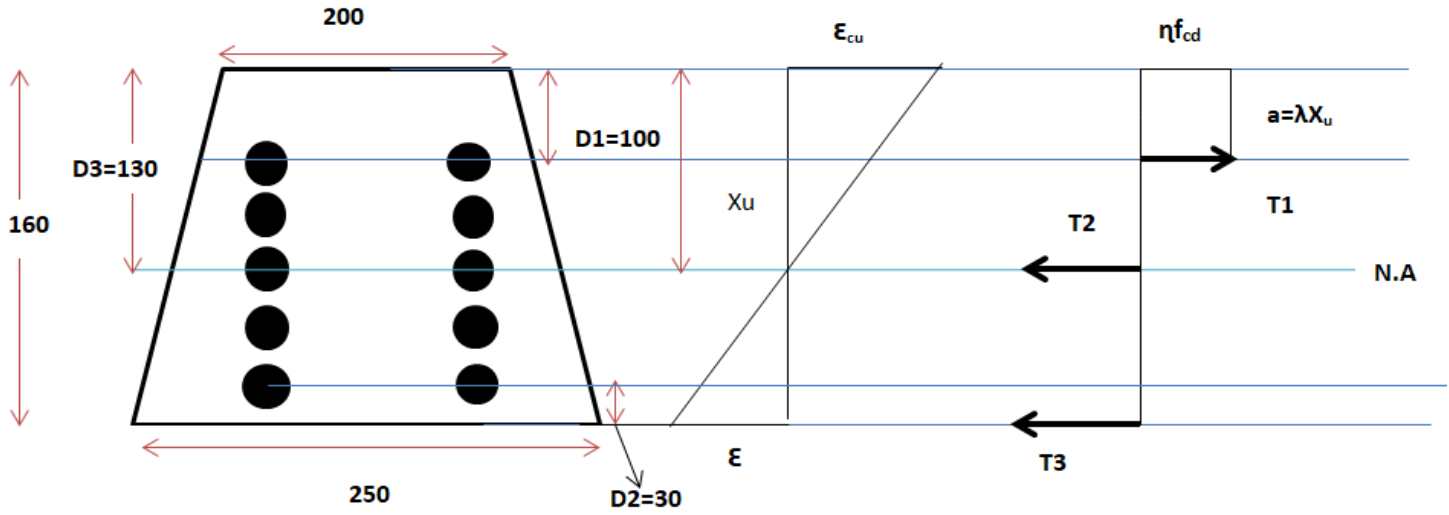

Figure 4.2: Conceptual diagrams for calculation bending strength of a sleeper

Where

N.A is neutral axis

Ɛcu is ultimate compressive strain in concrete

f_{cd} is design value of concrete compressive strength

T_1, T_2, T_3 are the forces in steel

X_u is the depth between the top line and neutral axis and is calculated by the centroid method

The trapezoidal shape is divided into three area

$$X_u = \frac{\sum A_i y_i}{\sum A_i} \qquad 4.3$$

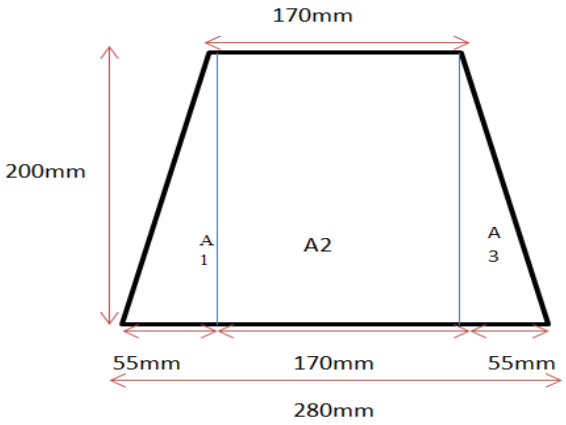

$$A_1 = A_3 = \frac{55 \times 200}{2} = 5500mm^2$$

$$A_2 = 170 \times 200 = 34000mm^2$$

At Rail Seat

$$X_u = \frac{\left(5500 \times \frac{200}{3}\right) + \left(34000 \times \frac{200}{2}\right) + \left(5500 \times \frac{200}{3}\right)}{5500 + 34000 + 5500} = 91.85mm$$

At Center

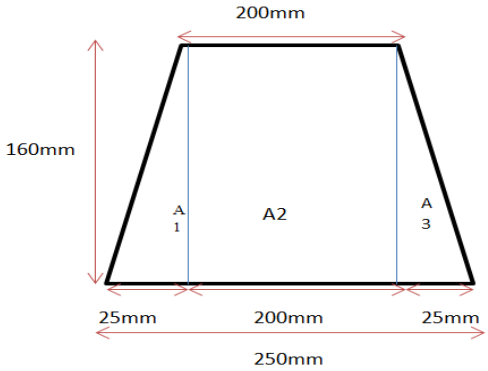

$$A_1 = A_3 = \frac{25 \times 160}{2} = 2000mm^2$$

$$A_2 = 160 \times 200 = 32000mm^2$$

$$X_u = \frac{\left(2000 \times \frac{160}{3}\right) + \left(32000 \times \frac{160}{2}\right) + \left(2000 \times \frac{160}{3}\right)}{2000 + 32000 + 2000} = 77.03mm$$

For rectangular stress distribution, the factor λ, defining the effective height of the compression zone and the factor η, defining the effective strength, are as expressed below

$$\lambda = \begin{cases} 0.8 & for\ f_{ck} \leq 50Mpa \\ 0.8 - \frac{(f_{ck} - 50)}{400} & for\ 50 \leq f_{ck} \leq 90MPa \end{cases} \quad 4.4$$

$$\eta = \begin{cases} 1 \quad for\ f_{ck} \leq 50MPa \\ 1 - \dfrac{(f_{ck} - 50)}{200} \quad for\ 50 \leq f_{ck} \leq 90MPa \end{cases} \tag{4.5}$$

f_{ck} =55MPa

$$\lambda = 0.8 - \frac{(55 - 50)}{400} = 0.7875$$

$$\eta = 1 - \frac{(55 - 50)}{200} = 0.975$$

Depth of compression zone
At rail seat $a = \lambda \times X_u = 0.7875 \times 91.85mm = 72.33mm$
At center $a = \lambda \times X_u = 0.7875 \times 77.03mm = 60.66mm.$

The compressive force of a simplified distance at the decompression zone is calculated by:

$$C = \alpha_c \times f_{cd} \times b \times d_{max} \tag{4.6}$$

$$\alpha_c = \frac{0.8X_u}{d} \tag{4.7}$$

Where C=compressive force, d_{max}=maximum distance at decompression reinforcement, b=width of section

f_{cd}=Design compressive strength of concrete

$$f_{cd} = \frac{\alpha_{cc} \times f_{ck}}{\gamma_c} = \frac{0.85 \times 55}{1.5} = 31.16MPa \tag{4.8}$$

Where γ_c is the partial factor of concrete, αcc is the coefficient taking account for longterm effects on the compressive strength and of unfavourabe effects depending on the way load is applied and for concrete γc is 1.5 (EN 1992-1-1 2004)

Take average value of width of sleeper for computation of compressive force
At rail-seat

$$k_x = \frac{X_u}{d} = \frac{91.85}{170} = 0.54 \tag{4.9}$$

$$\alpha_c = 0.8 \times k_x = 0.8 \times 0.54 = 0.432 \tag{4.10}$$

$$\boldsymbol{C = 0.432 \times 31.16 \times 280 \times 170 = 640.75kN}$$

At center

$$k_x = \frac{X_u}{d} = \frac{77.03}{130} = 0.592 \quad (4.11)$$

$$\alpha_c = 0.8 \times k_x = 0.8 \times 0.592 = 0.474 \quad (4.12)$$

$$C = 0.474 \times 31.16 \times 250 \times 130 = 480.02kN$$

4.1.1.2 Tension forces of steel bars

The tension forces from steel bars can be estimated by

$$T_n = \varepsilon_{tn} \times E_p \times A_p \times n_i \quad (4.13)$$

Where

ε_{tn} is the total strain of single steel bar on n^{th} row

E is the Young's modulus of steel bars

A_p is the area of steel bar

n_i is the number of steel bars in n^{th} row

Strain in prestressing steel at transfer (ε_{pt})

$$\varepsilon_{pt} = \frac{f_{pt}}{E_p} \quad (4.14)$$

Where f_{pt} is allowable stress of steel, Ep is Young's modulus of steel

$$\varepsilon_{ct} = \frac{1}{E_c}\left(\frac{P_t}{A} + \frac{P_t(d_{max} - y_t)^2}{I}\right) \quad (4.15)$$

Where

A is the area of the cross-section

D_{max} is lowest level of steel in the compression zone

Y_t is the centroid from top or bottom

E_C is Young's modulus of concrete

I is moment of inertia

The stress at failure corresponding to the total strain

$$f_p = \begin{cases} \varepsilon_p \times \varepsilon_{pu}, if\ \varepsilon_{pu} \le 0.0076 \\ 1860\ MPa - \dfrac{0.3Mpa}{\varepsilon_{pu} - 0.0064}, \quad if \varepsilon_{pu} \ge 0.0076 \end{cases} \qquad 4.16$$

Apply similarity of triangle to find strain

At Rail seat

$$\varepsilon_{pt} = \frac{0.75 \times 1860}{200000} = 0.007$$

From top of the sleeper

$$\varepsilon_{ct} = \frac{1}{37000}\left(\frac{429660}{45000} + \frac{429660(170 - 108.15)^2}{143.65 \times 10^6}\right) = 0.0006$$

$$\varepsilon_{ct1} = \frac{\varepsilon_{ct}(y_t - d_1)}{d_{max} - y_t} = \frac{0.0006(108.15 - 100)}{170 - 108.15} = 0.00008$$

$$\varepsilon_{ct2} = \frac{\varepsilon_{ct}(y_t - d_2)}{d_{max} - y_t} = \frac{0.0006(108.15 - 130)}{170 - 108.15} = -0.00021$$

$$\varepsilon_{ct3} = \frac{\varepsilon_{ct}(y_t - d_3)}{d_{max} - y_t} = \frac{0.0006(108.15 - 170)}{170 - 108.15} = -0.0006$$

Assume concrete strain (ε_{cu})= 0.0035

$$\varepsilon_{cpu1} = \frac{\varepsilon_{cu}(d_1 - X_u)}{X_u} = \frac{0.0035(100 - 73.48)}{73.48} = 0.0013$$

$$\varepsilon_{cpu2} = \frac{\varepsilon_{cu}(d_2 - X_u)}{X_u} = \frac{0.0035(130 - 73.48)}{73.48} = 0.0027$$

$$\varepsilon_{cpu3} = \frac{\varepsilon_{cu}(d_3 - X_u)}{X_u} = \frac{0.0035(170 - 73.48)}{73.48} = 0.0046$$

Summation of strain components

$$\varepsilon_{pu1} = \varepsilon_{pt} + \varepsilon_{ct1} + \varepsilon_{cpu1} = 0.007 + 0.0006 + 0.0013 = 0.0084$$

$$\varepsilon_{pu2} = \varepsilon_{pt} + \varepsilon_{ct2} + \varepsilon_{cpu2} = 0.007 - 0.00021 + 0.0027 = 0.0095$$

$$\varepsilon_{pu3} = \varepsilon_{pt} + \varepsilon_{ct3} + \varepsilon_{cpu3} = 0.007 - 0.0006 + 0.0046 = 0.011$$

The stress at failure corresponding to the total strain is the following:

$$f_{p1} = 1860 - \frac{0.3}{0.0084 - 0.0064} = 1710MPa$$

$$f_{p2} = 1860 - \frac{0.3}{0.0095 - 0.0064} = 1763.2MPa$$

$$f_{p3} = 1860 - \frac{0.3}{0.011 - 0.0064} = 1795MPa$$

The corresponding tensile forces:

$$T_1 = A_{P1} \times f_{p1} = 115.5 \times 1710 = 197.505kN$$

$$T_2 = A_{P2} \times f_{p2} = 77 \times 1763.2 = 135.766kN$$

$$T_3 = A_{P3} \times f_{p3} = 115.5 \times 1795 = 207.322kN$$

$$T = T_1 + T_2 + T_3 = (197.505 + 135.766 + 207.322)kN = 540.593kN$$

At Center

$$\varepsilon_{pt} = \frac{0.75 \times 1860}{200000} = 0.007$$

From top of the sleeper

$$\varepsilon_{ct} = \frac{1}{37000}\left(\frac{429660}{36000} + \frac{429660(130 - 85.85)^2}{68.84 \times 10^6}\right) = 0.00065$$

$$\varepsilon_{ct1} = \frac{\varepsilon_{ct}(y_t - d_1)}{d_{max} - y_t} = \frac{0.00065(85.85 - 60)}{130 - 85.85} = 0.00038$$

$$\varepsilon_{ct2} = \frac{\varepsilon_{ct}(y_t - d_2)}{d_{max} - y_t} = \frac{0.00065(85.85 - 90)}{130 - 85.85} = -0.00061$$

$$\varepsilon_{ct3} = \frac{\varepsilon_{ct}(y_t - d_3)}{d_{max} - y_t} = \frac{0.00065(85.85 - 130)}{130 - 85.85} = -0.00065$$

Assume concrete strain (ε_{cu})= 0.0035

$$\varepsilon_{cpu1} = \frac{\varepsilon_{cu}(d_1 - X_u)}{X_u} = \frac{0.0035(60 - 61.62)}{61.62} = -0.000092$$

$$\varepsilon_{cpu2} = \frac{\varepsilon_{cu}(d_2 - X_u)}{X_u} = \frac{0.0035(90 - 61.62)}{61.62} = 0.0016$$

$$\varepsilon_{cpu3} = \frac{\varepsilon_{cu}(d_3 - X_u)}{X_u} = \frac{0.0035(130 - 61.62)}{61.62} = 0.00388$$

Summation of strain components

$$\varepsilon_{pu1} = \varepsilon_{pt} + \varepsilon_{ct1} + \varepsilon_{cpu1} = 0.007 + 0.00038 - 0.000092 = 0.0073$$

$$\varepsilon_{pu2} = \varepsilon_{pt} + \varepsilon_{ct2} + \varepsilon_{cpu2} = 0.007 - 0.00061 + 0.0016 = 0.0079$$

$$\varepsilon_{pu3} = \varepsilon_{pt} + \varepsilon_{ct3} + \varepsilon_{cpu3} = 0.007 - 0.00065 + 0.00388 = 0.01023$$

The stress at failure corresponding to the total strain is the following:

$$f_{p1} = 1860 - \frac{0.3}{0.0073 - 0.0064} = 1527MPa$$

$$f_{p2} = 1860 - \frac{0.3}{0.0079 - 0.0064} = 1660MPa$$

$$f_{p3} = 1860 - \frac{0.3}{0.01023 - 0.0064} = 1782MPa$$

The corresponding tensile forces:

$$T_1 = A_{P1} \times f_{p1} = 115.5 \times 1527 = 176.36kN$$

$$T_2 = A_{P2} \times f_{p2} = 77 \times 1660 = 127.820kN$$

$$T_3 = A_{P3} \times f_{p3} = 115.5 \times 1782 = 205.82kN$$

$$T = T_1 + T_2 + T_3 = (176.36 + 127.820 + 205.82)kN = 510kN$$

Using PolyBeam software, bending moment and shear force have been determined with different pressure distribution as it is shown below

A. In the analysis, The Australian standard consider for 50% uniform pressure at the center of the sleeper, while China standard accounts for 75% uniform pressure at the center of the sleeper. In this thesis, the design bending moment is calculated using the center-binding coefficient of 0.5 and 0.75

Rail seat load

$$R = \frac{125 * 250 * 0.52}{100} = 162.5kN$$

Therefore the assumed uniformly distributed load *w* (kN/m) over the entire sleeper length *l* (m) is

$$W = \frac{2 \times 162.5}{2.5} = 130kN/m$$

1. **Moment at Rail seat**

- **Rail seat positive bending moment**

$$M_{R^+} = \frac{R(l-g)}{8} \qquad 4.17$$

$$M_{R^+} = \frac{162.5(2.5-1.51)}{8} = 20.1\ kNm$$

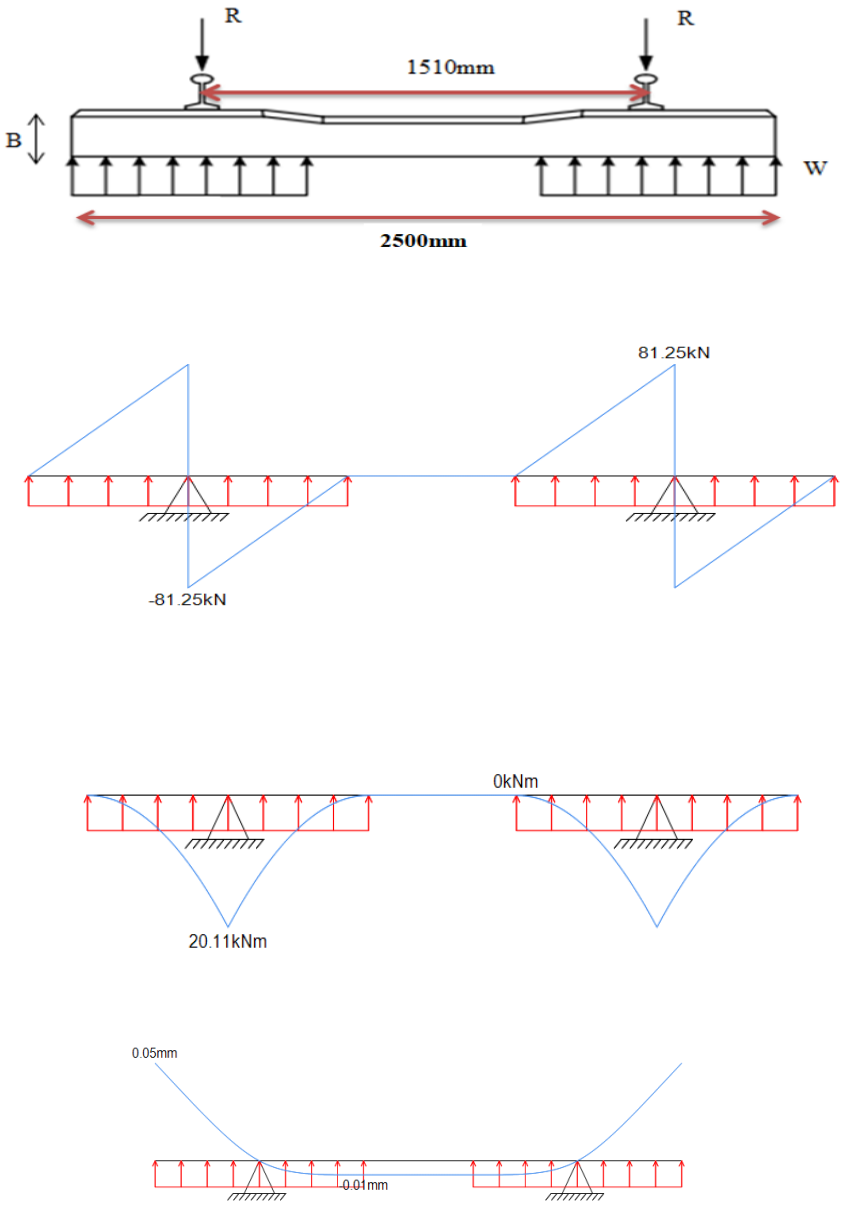

Figure 4.3 Shear force, bending moment and deflection diagrams for zero center binding ballast pressure

- **Rail seat negative bending moment**

The rail seat negative bending moment M_{R-} shall not be less than 67% of the rail seat positive bending moment M_{R+} or 14 kNm whichever greater

$$M_{R^-} = \max of\ (0.67 \times 20.1) = 13.5kNm < 14kNm = 14kNm$$

2. Moment at the center

- ***Center positive design bending moment (****a=0.9(l-g))*

$$M_{C^+} = 0.05 \times R(l - g) \qquad 4.18$$

$$M_{C^+} = 0.05 \times (2.5 - 1.51) = 8.04375kNm$$

- **Center Negative design bending moment**

  The maximum negative bending moment has been taken to occur at the center of the sleeper . In this case totally and partially distribution ballast pressure are considered.

  This maximum center bending moment (M_C) with uniform distribution ballast pressure is determined by the following equation:

$$M_{C^-} = \frac{R(2g - l)}{4} \qquad 4.19$$

$$M_{C^-} = \frac{162.5(2 \times 1.51 - 2.5)}{4} = 21.12kNm$$

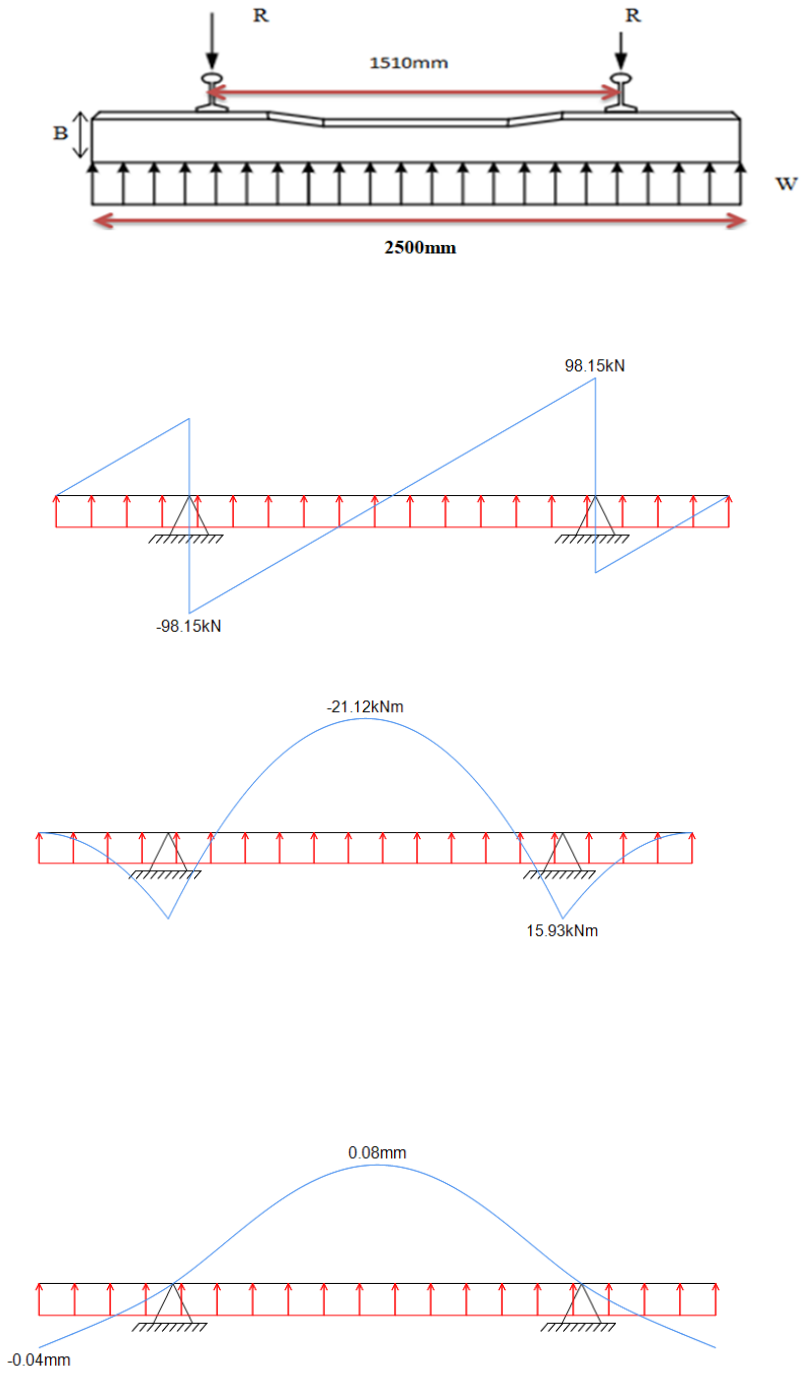

Figure 4.4 Shear force , bending moment and deflection diagrams for 100% of center binding coefficient

For partially distribution ballast pressure AS 1085.14 accounts 50% the uniform pressure and 75% in china's standard case were analyzed.
For this analysis the center binding coefficient are 0.75 and 0.5

α=75%

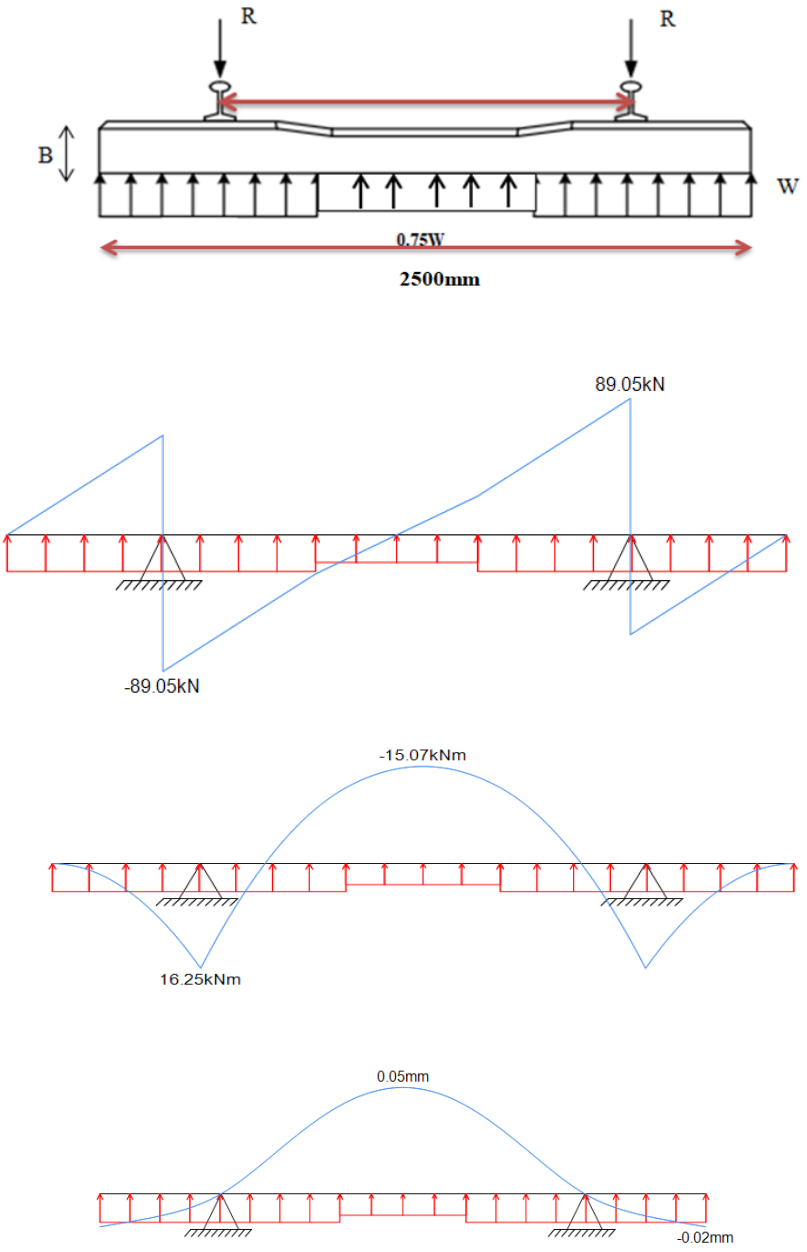

Figure 4.5 Shear force, bending moment and deflection diagrams for 75% of center binding coefficient

α=50%

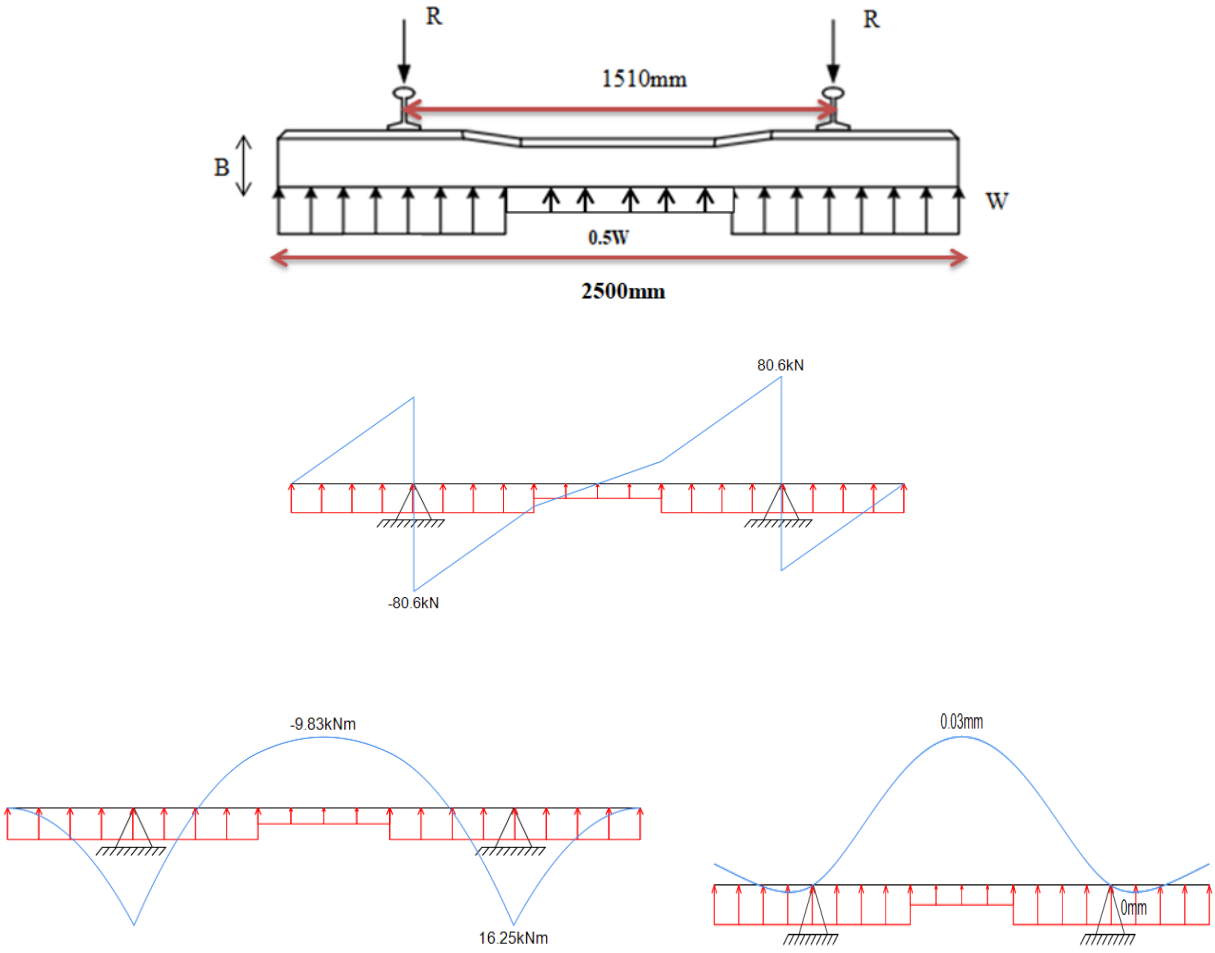

Figure 4.6 Shear force and bending moment diagrams for 50% center binding coefficient

Table 4.2 Summary of results for different ballast distribution pressure at the center of the sleeper

Support condition	Shear force(kN)		Maximum Bending moment (kNm)		Deflection(mm)	
	Rail seat	center	Rail seat	center	Rail seat	center
Full supported	98.15	0	15.93	21.12	-0.04	0.08
75% supported	89.05	0	16.25	15.07	-0.02	0.05
50 supported	80.06	0	16.25	9.83	0	0.03

Table 4.2 shows that once ballast distribution pressure reduces at the centre of the sleeper with 75% and 50%, at rail seat bending moments increase 2% while shear force decrease with 9.3% and 18.43% respectively and deflection decrease with 50% and 100% respectively similar to the centre of the sleeper the results show bending moment decrease with 28.6% and 53.4% respectively and deflection decrease with 37.5%, 62.5% respectively.

B. Ballast pressure distribution with 75%, 50% and 25% reductions under rail seat analysis

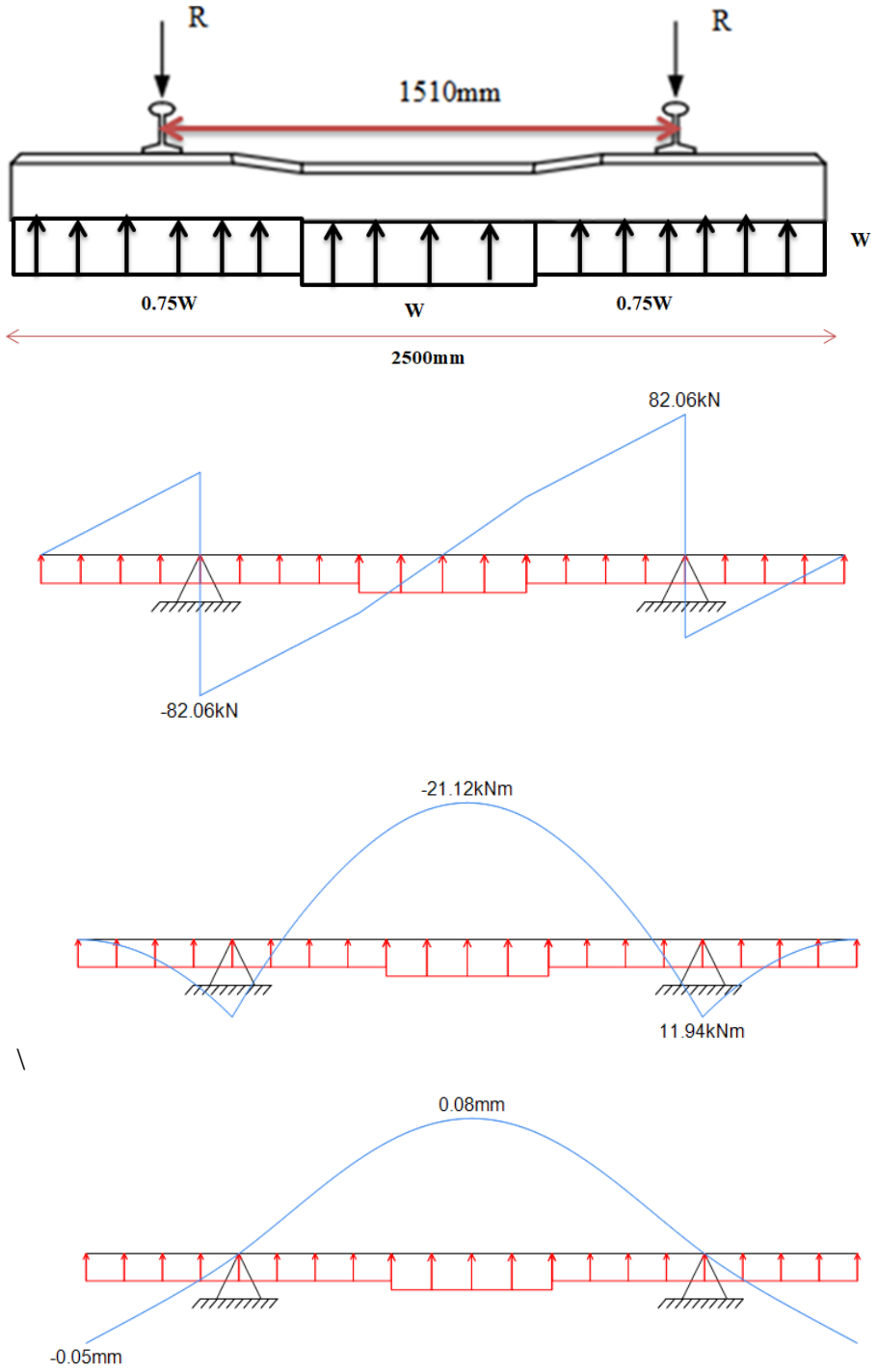

Figure 4.7 Shear force and bending moment diagrams for 75% of ballast distribution pressure under rail seat

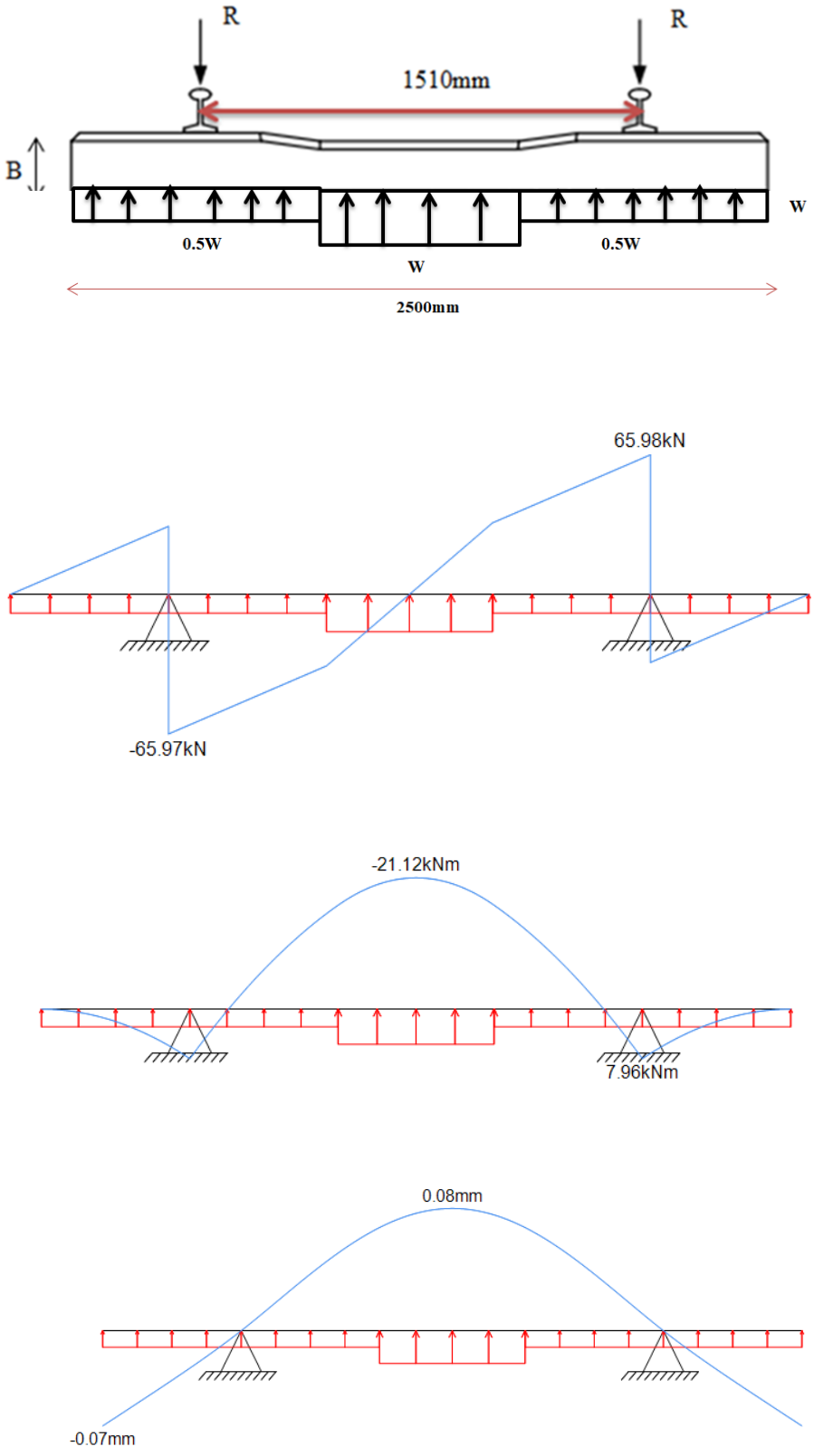

Figure 4.8 Shear force and bending moment diagrams for 50% of ballast distribution pressure under rail seat

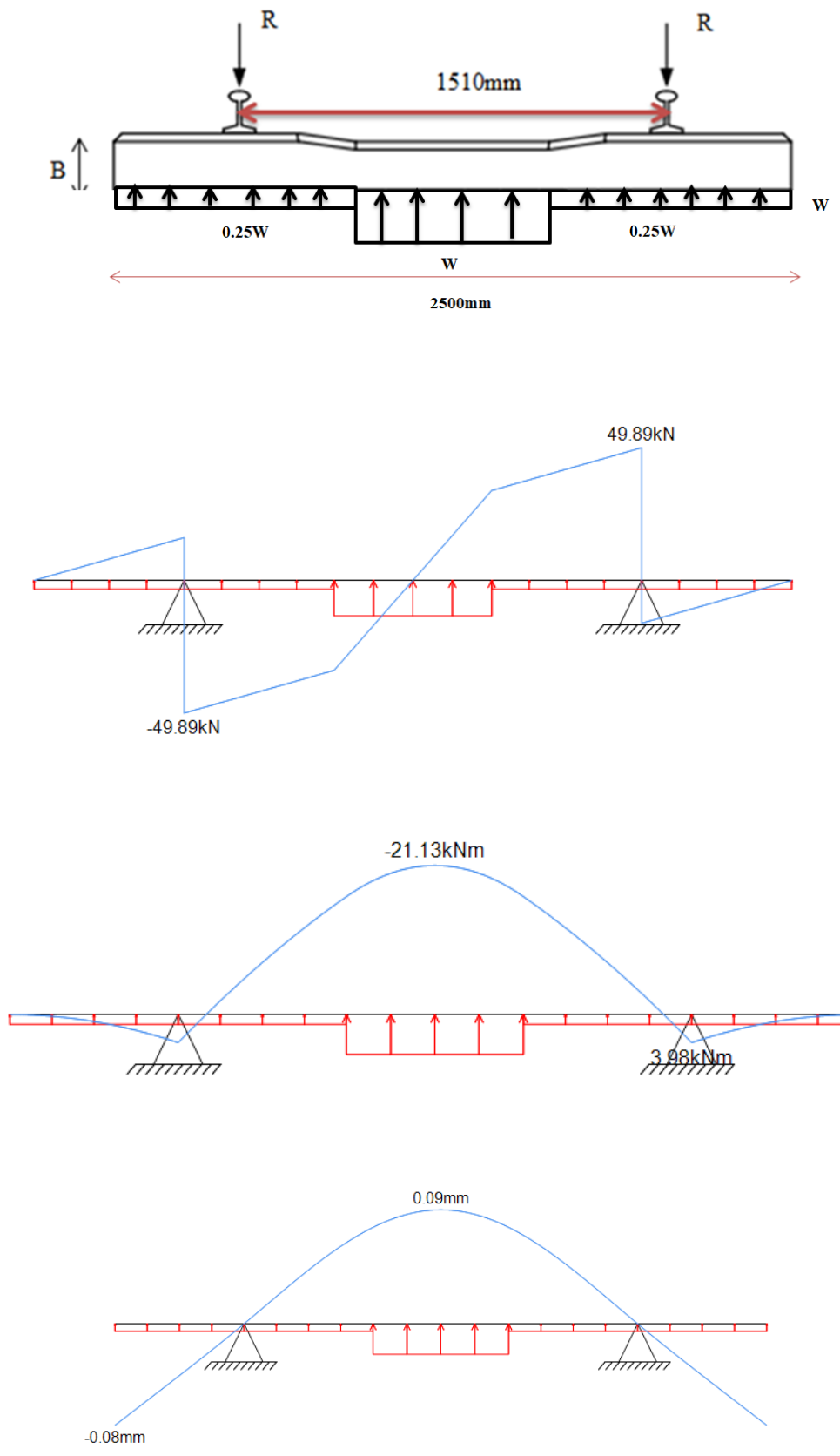

Figure 4.9 Shear force and bending moment diagrams for 25% of ballast distribution pressure under rail seat

Table 4.3 Summary of results for different ballast distribution pressure under rail seat

Support condition	Shear force(kN)		Bending moment (kNm)		Deflection(mm)	
	Rail seat	center	Rail seat	center	Rail seat	center
100%(Full supported)	98.15	0	15.93	21.12	-0.04	0.08
75% supported	82.06	0	11.94	21.12	-0.05	0.08
50% supported	65.98	0	7.96	21.12	-0.07	0.08
25% supported	49.89	0	3.98	21.13	-0.08	0.09

Table 4.3 shows that once ballast distribution pressure reduces under the rail seat of the sleeper with 75% 50% and 25% at rail seat, bending moments decrease with 25%, 50% and 75% respectively while shear force decrease with 16.4% , 32.7% and 49.2% respectively and while at the center of the sleeper shear force, bending moment and deflection remain constant.

.

Considering elastic support

Using BOEF (Beam On Elastic Foundation) spreadsheet developed by Alex Tomanovich , the sleeper on elastic support was analysed by computing ,shear force ,bending moment and deflections

BEAM ON ELASTIC FOUNDATION ANALYSIS

For Soil Supported Beam, Combined Footing, Slab Strip or Mat Strip of Assumed Finite Length with Both Ends Free

Job Name:		Subject:			
Job Number:		Originator:		Checker:	

Input Data:

Beam Data:

Length, L =	2.5000	m
Width, B =	0.1900	m
Thickness, T =	0.2200	m
Modulus, E =	37000	MPa
Subgrade, ks =	250	MN/m

Beam Loadings:

Full Uniform:

	Start		End	
Distributed:	b (m)	Wb (kN/m)	e (m)	We (kN/m)
#1:				
#2:				
#3:				
#4:				
#5:				
#6:				

Point Loads:	a (m)	P (kN)
#1:	0.4950	162.50
#2:	2.0050	162.50
#3:		
#4:		
#5:		
#6:		
#7:		
#8:		
#9:		
#10:		
#11:		
#12:		

Results:

Beam Flexibility Criteria:

for β*L <= π/4	beam is rigid
for π/4 < β*L < π	beam is semi-rigid
for β*L >= π	beam is flexible
for β*L >= 6	beam is semi-infinite long

Inertia, I =	0.00017	m^4	I = B*T^3/12
β =	0.209		β = ((ks*B)/(4*E*I))^(1/4)
β*L =	0.522		β*L = Flexibility Factor

Beam is rigid

Max. Shears and Locations:

+V(max) =	98.14	kN	@ x =	2.01	m
-V(max) =	-98.14	kN	@ x =	0.50	m

Max. Moments and Locations:

+M(max) =	15.96	kN-m	@ x =	0.50	m
-M(max) =	-22.23	kN-m	@ x =	1.25	m

Max. Deflection and Location:

Δ(max) =	0.042	mm	@ x =	0.00	m

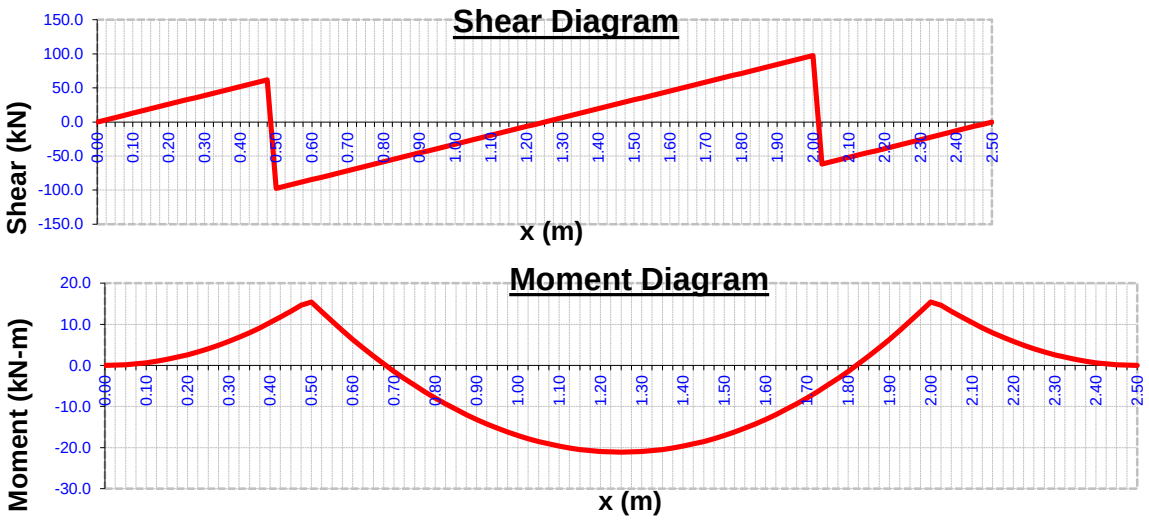

Figure 4.10 Shear force and bending moment diagrams for uniformly elastic support

Table 4.4 Comparison of Polybeam and BOEF results for full uniformly supported

	RAIL SEAT			CENTER		
	M_{max}+ (kNm)	V_{max} (kN)	D_{max} (mm)	M_{max}- (kNm)	V_{max}(kN)	D_{max} (mm)
Polybeam	15.93	98.15	-0.04	21.12	0	0.08
BOEF	15.96	98.14	-0.042	22.23	0	0.0845
Percentage difference (%)	0.18%	0.01%	4.9%	5.12%	0	17.6%

4.2 Static modelling of Prestressed Concrete Sleeper on Elastic Support

In chapter three, the structure, material properties, elements, and parameters used in modeling are illustrated. The prestressed concrete sleeper was analyzed using ABAQUS through static structural analysis. The analysis results of all models are presented and statically analyzed in this section to obtain the deformation and stresses.

The results for full supported ballast (250MN/m)

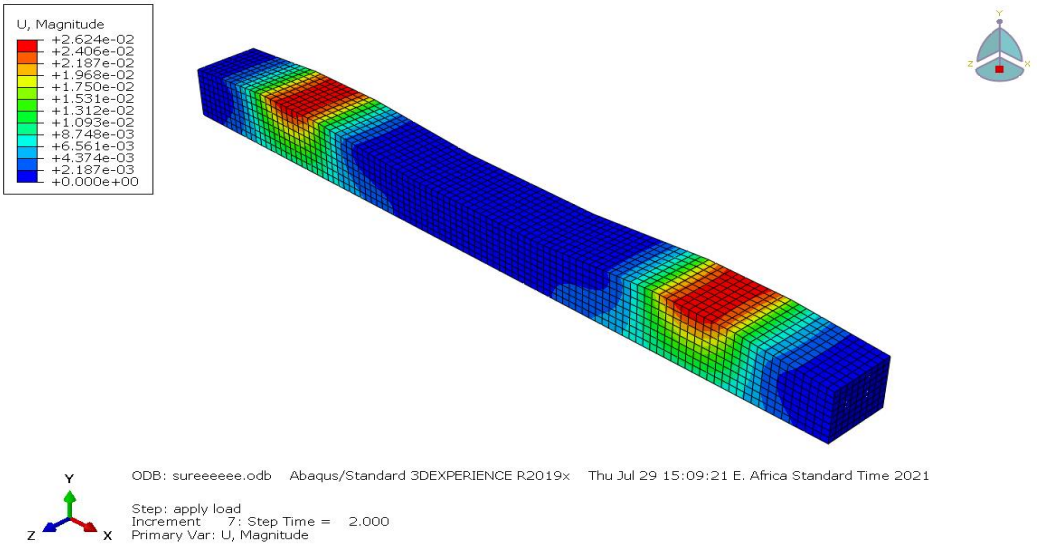

Figure 4.11 Total displacement along the sleeper

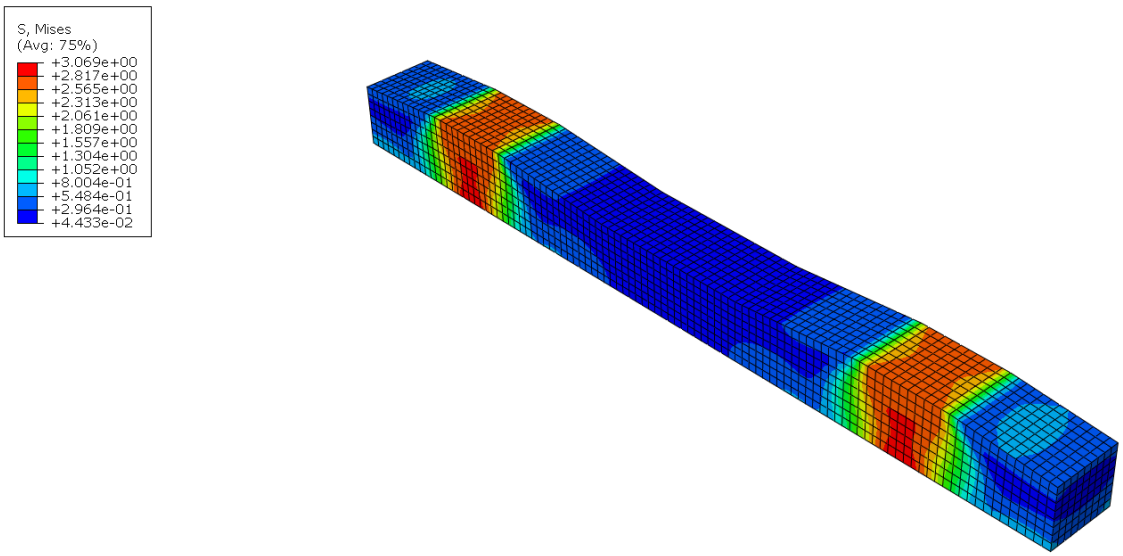

Figure 4.12 Von mises stress along the sleeper

Displacement

The degree to which a structure's element changes shape when a load is applied is referred to as displacement. The change can be a distance or an angle, and it can be visible or invisible, depending on the load intensity, the shape of the component, and the material from which it is made.

Displacement results in ABAQUS are typically obtained as either total displacement or directional displacement.

In this study, Critical sections such as the rail seat, center, and end sections have been highlighted, and the rail seat section has the greatest deformation.

In this study, *Ks* = total ballast stiffness per sleeper, equals to 250 MN / m[71]

1. Total displacement results are displayed for different distribution coefficient ballast stiffness at the center of the sleeper and incremental percentage for displacement has been calculated

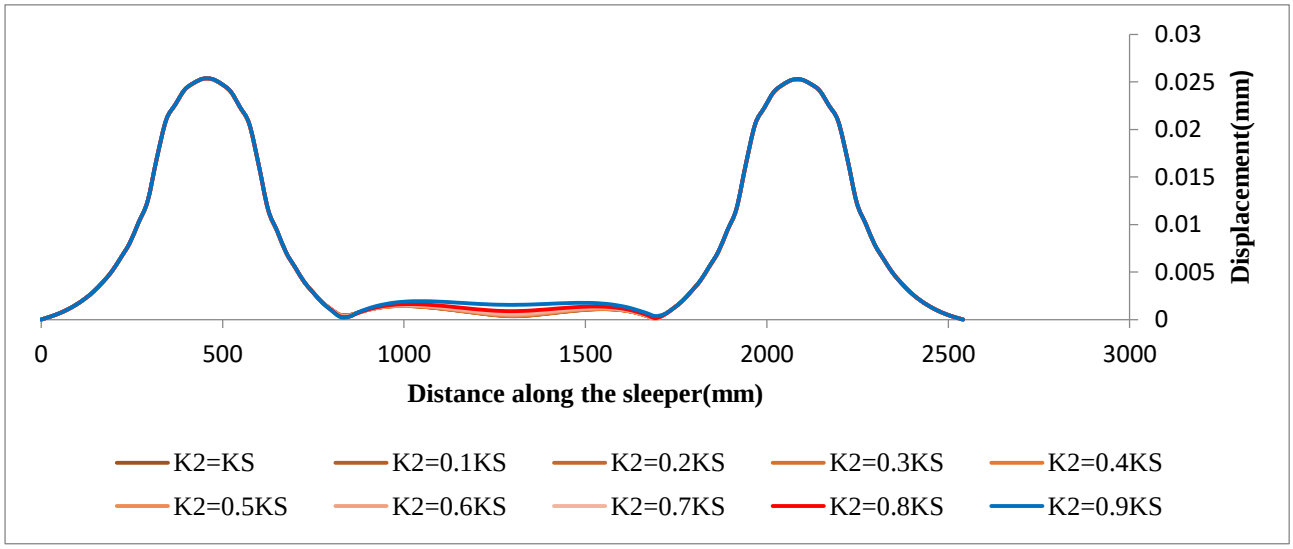

Figure 4.13 Total displacement along the sleeper

Table 4.5 Incremental percentage with change of ballast stiffness at the center of the sleeper

Distribution coefficient	Incremental%	Distribution coefficient	Incremental%
0.1	0.091	0.6	0.016
0.2	0.051	0.7	0.012
0.3	0.036	0.8	0.008
0.4	0.024	0.9	0.004
0.5	0.020	1	0.000

Figure 4.13 shows that there is a small variation of displacement It is highlighted when ballast stiffness as support reduce at the centre of the sleeper from 100% to 90%,80%.70%,60%,50%,40%.30%, 20%, and 10% and table 4.5 shows that the displacement of the sleeper increased a small portion of (0.004%-0.091%) more than 100% supported and much more displacement occur at the rail seat.

Therefore, once the ballast stiffness reduce at the center of the sleeper there is a small increase in displacement but to keep the performance of the sleeper, the low ballast stiffness at the center of the sleeper should be avoided

2. Displacement results are displayed for different ballast stiffness variation along the sleeper which are: 250MN/m, 225MN/m, 200MN/m, 175MN/m, 150MN/m, 125MN/m and 62.5 MN/m and results are highlighted.

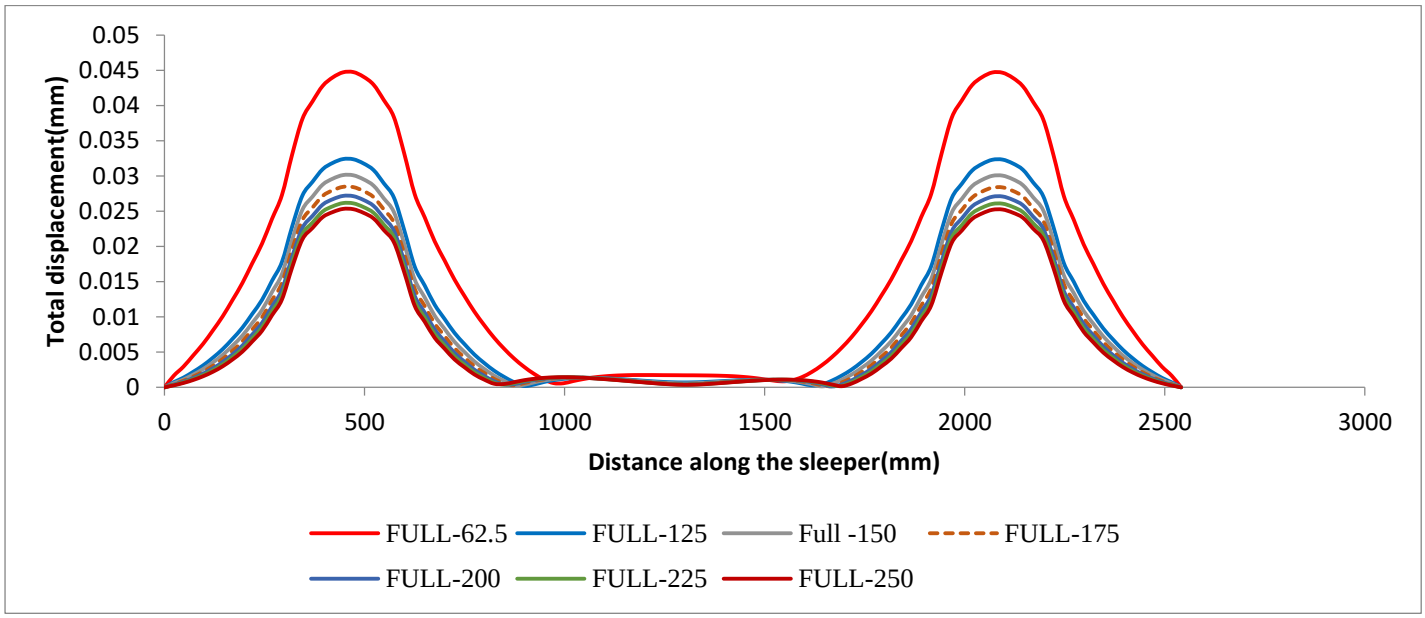

Figure 4.14 Displacement for ballast stiffness variation along the sleeper

Table 4.6 Incremental percentage stiffness variation of displacement for ballast along the sleeper

Stiffness(MN/m)	Max displacement(mm)	Incremental percentage(%)
62.5	0.045	76.7
125	0.032	27.94
150	0.030	18.97
175	0.028	12.37
200	0.027	7.29
225	0.026	3.27
250	0.025	0

Figure 4.14 shows the graph of displacement along the sleeper and once the ballast stiffness reduce along the sleeper from 100% supported (full supported) to 90%, 80%, 70%, 60%, 50% and 25% supported, there is a significant increase of the displacement when the sleeper is supported at 25 and 50 % and table 4.6 shows that the incremental percentage increased with 3.27%, 7.29%, 12.37%, 18.97%, 27.94% and 76.7% respectively more than full supported. Therefore, when there is high ballast stiffness reduction along the sleeper, there is more increasing in displacement.

Third result: Total displacement results are displayed for different ballast stiffness variation along the sleeper with center ballast stiffness reduction in percentage which are: 90%, 80%, 70%, 60% and 50% and results from different stiffness reduction are highlighted.

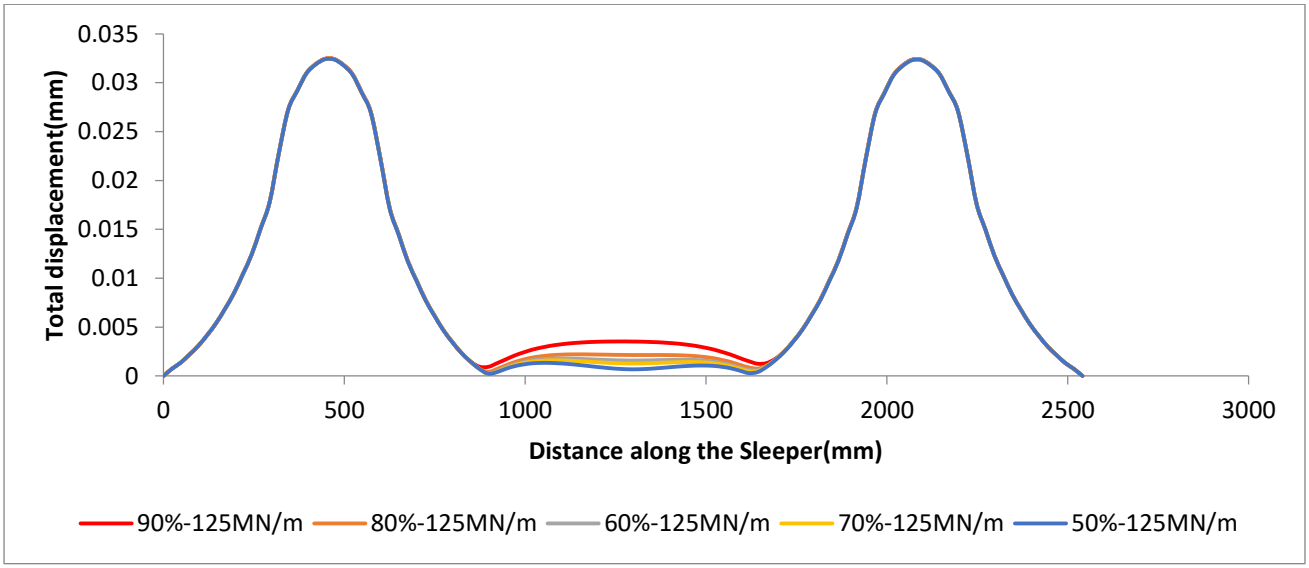

Figure 4.15 comparison of displacement for ballast stiffness variation along the sleeper

As it is highlighted with Figure 4.15, the graph shows that when stiffness is reduced at the middle of the sleeper with reduction percentage of 50%, 60%,70%,80% and 90% ,the displacement increased with a small portion of 1.2%, 1.28% ,1.29%, 1.32% and 1.4% respectively .There is a small portion of increase that cannot affect the sleepers

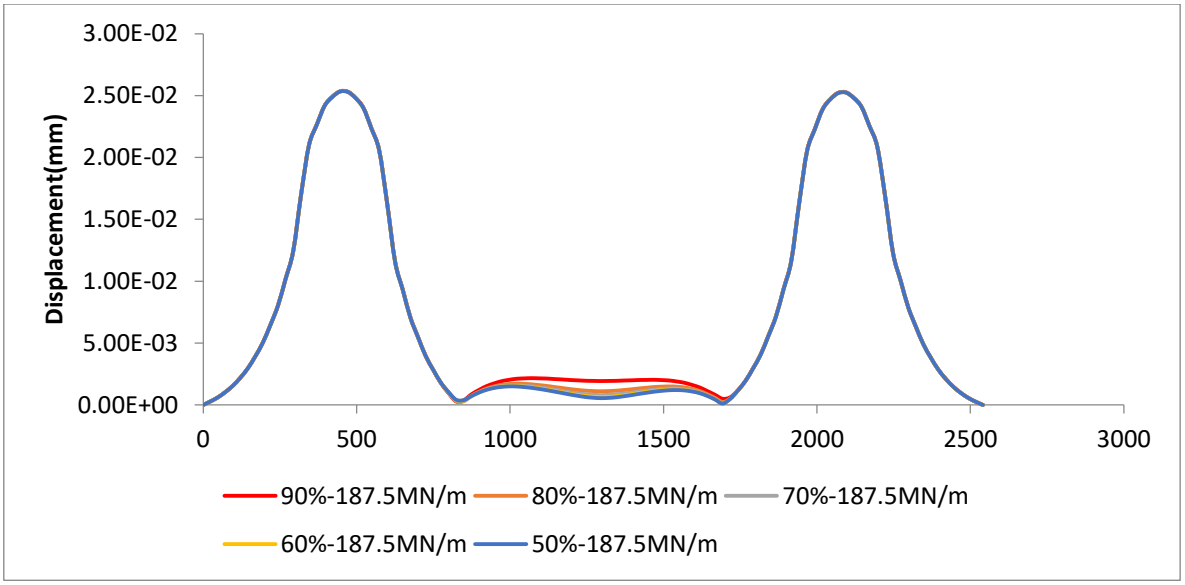

Figure 4.16 comparison displacement for ballast stiffness along the sleeper

As it is highlighted in below figure 4.16, when stiffness is reduced at the middle of the sleeper with reduction percentage of 50%,60%,70%,80% and 90% ,the displacement increased with a small portion of 0.01%, 0.046% ,0.05%, 0.079% and 0.13% respectively

Von-Mises stress

The von Mises stress is a value that is used to determine whether a given material will yield or fracture. It is typically applied to ductile materials such as metals. According to the Von Mises yield criterion, if a material's von mises stress under load is equal to or greater than its yield limit under simple tension, the material will yield. As it is shown in the following Figures the results are displayed in curves in three parts

1.Von mises stress results are displayed for different distribution coefficient ballast stiffness at the center of the sleeper which are, 1, 0.9,0.8,0.7,0.6,0.5,0.4,0.3,0.2,and 0.1 corresponding to250MN/m,225MN/m,200MN/m,175MN/m,150MN/m,125MN/m,100MN/m,75MN/m,50MN/m and 25MN/m respectively and results from different stiffness reduction are highlighted.

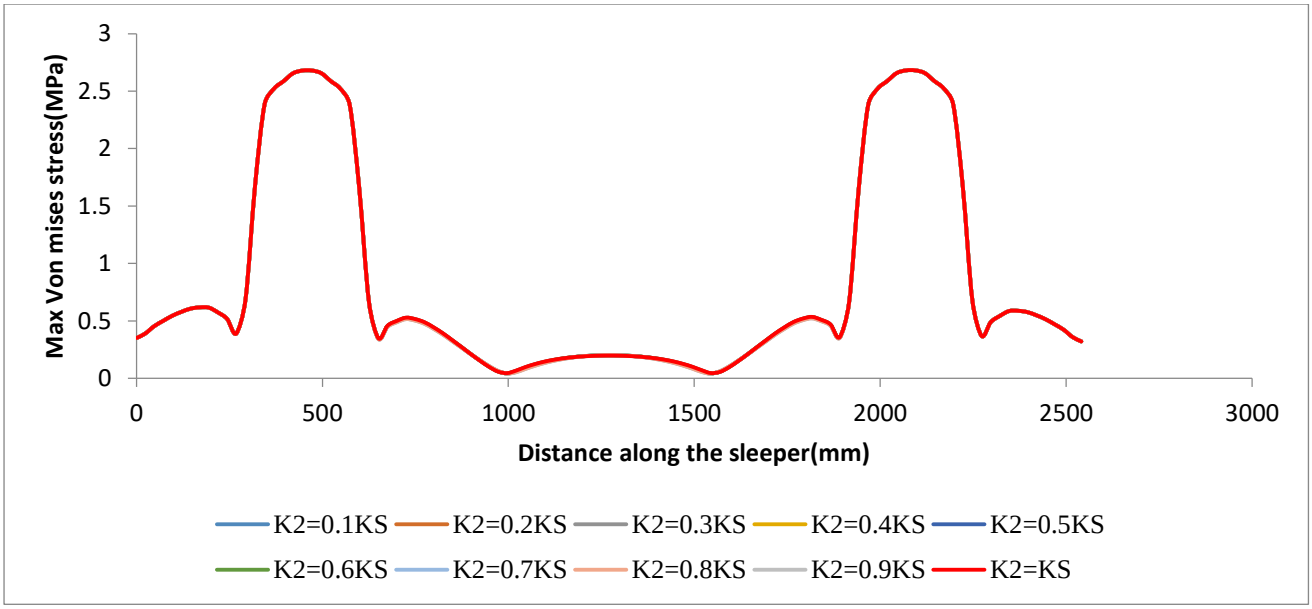

Figure 4.17 Von Mises Stress of ballast stiffness variation at the middle of the sleeper

Table 4.7 Incremental percentage of von mises stress for ballast stiffness reduction at the center of the sleeper

case	Max von mises stress(MPa)	Increment percentage (%)
K2=0.1KS	2.68186	0.07
K2=0.2KS	2.68132	0.05
K2=0.3KS	2.68109	0.04
K2=0.4KS	2.68096	0.035
K2=0.5KS	2.68087	0.033
K2=0.6KS	2.68082	0.031
K2=0.7KS	2.68077	0.029
K2=0.8KS	2.68074	0.028
K2=0.9KS	2.68071	0.027
K2=1KS	2.68	0

It is highlighted with the figure 4.17 that when ballast stiffness reduce at the centre of the sleeper from 100%(full supported) to 90%,80%.70%,60%,50%,40%.30%, 20%, and 10% supported , there is an insignificant variation along the sleepers for all reductions and table 4.7 von mises stress of the sleeper increased a small portion of (0.027%-0.07%) more than 100% supported and much more stress occured at the rail seat.

Therefore, once the ballast stiffness reduce at the center of the sleeper there is a small increase in stress but to keep the performance of the sleeper, the low ballast stiffness at the center of the sleeper should be avoided.

2. Von mises stress results are displayed for different ballast stiffness variation along the sleeper which are:250MN/m,187.5MN/m,175MN/m, 150MN/m, 125MN/m and 62.5 MN/m and results from different stiffness reduction are highlighted.

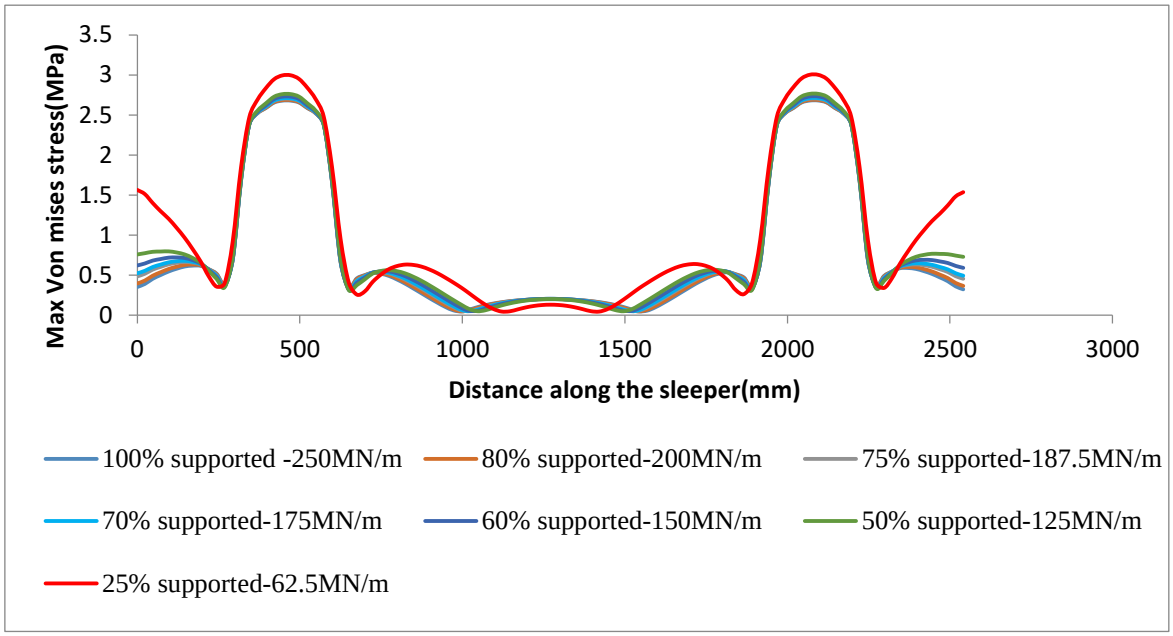

Figure 4.18: Von Mises Stress of ballast stiffness variation along the sleeper

Figure 4.18 shows the graph of von mises stresses along the sleeper and once the ballast stiffness reduce along the sleeper from 100% supported (full supported) to 80% , 70%, 60% ,50% and 25% supported , the von mises stresses increased with 0.28%, 0.86%, 1.06%, 1.062%, 3.12% and 12.04% respectively more than full supported . It is clear that the stresses increased with a small portion that is insignificant to affect the performance of sleeper.

3. KS =125MN/m, von mises stress results are displayed for different ballast stiffness variation along the sleeper with center ballast stiffness reduction in percentage which are: 90%, 80%, 70%, 60% and 50% and results from different stiffness reduction are highlighted.

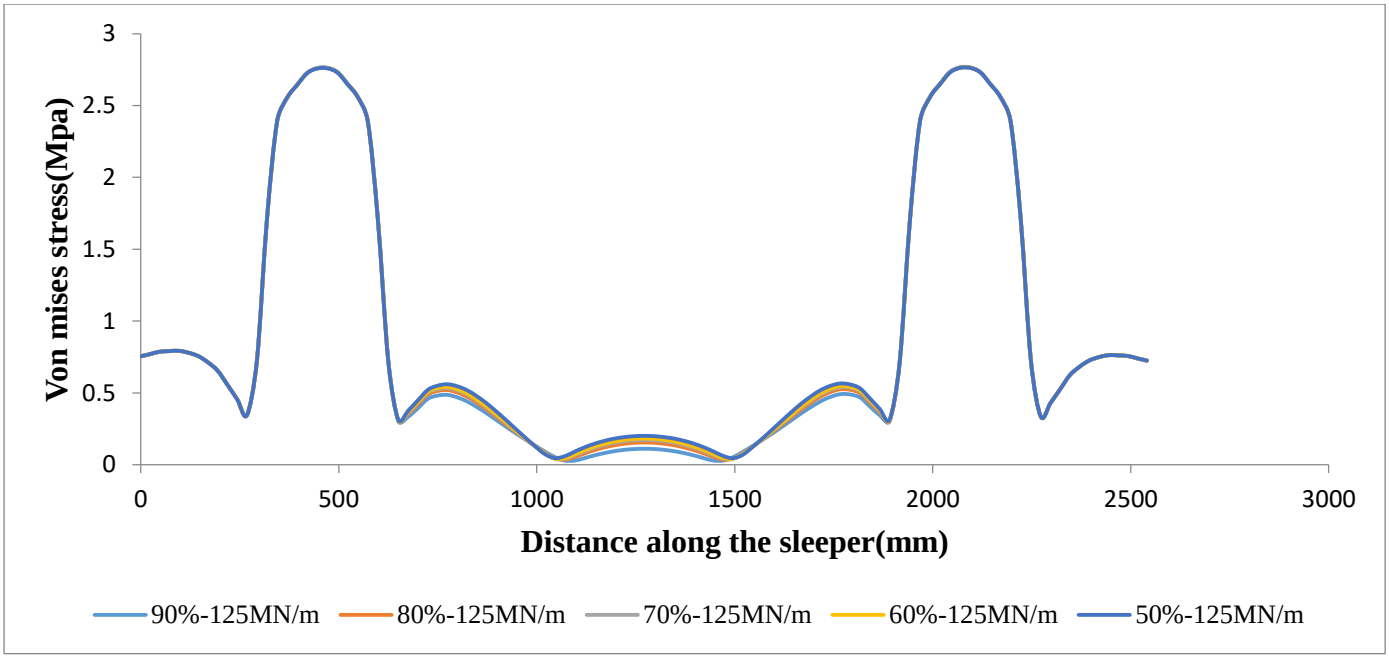

Figure 4.19 Von Mises Stress of ballast stiffness variation along the sleeper

It is highlighted with the figure 4.19 that when ballast stiffness reduce at the centre of the sleeper from 100% to 90%,80%.70%,60%, and 50%, supported , the von mises stress of the sleeper increased a small portion of (0.0007%-0.16%) more than 100% supported ,therefore this reduction will not cause too much stress on the sleeper.

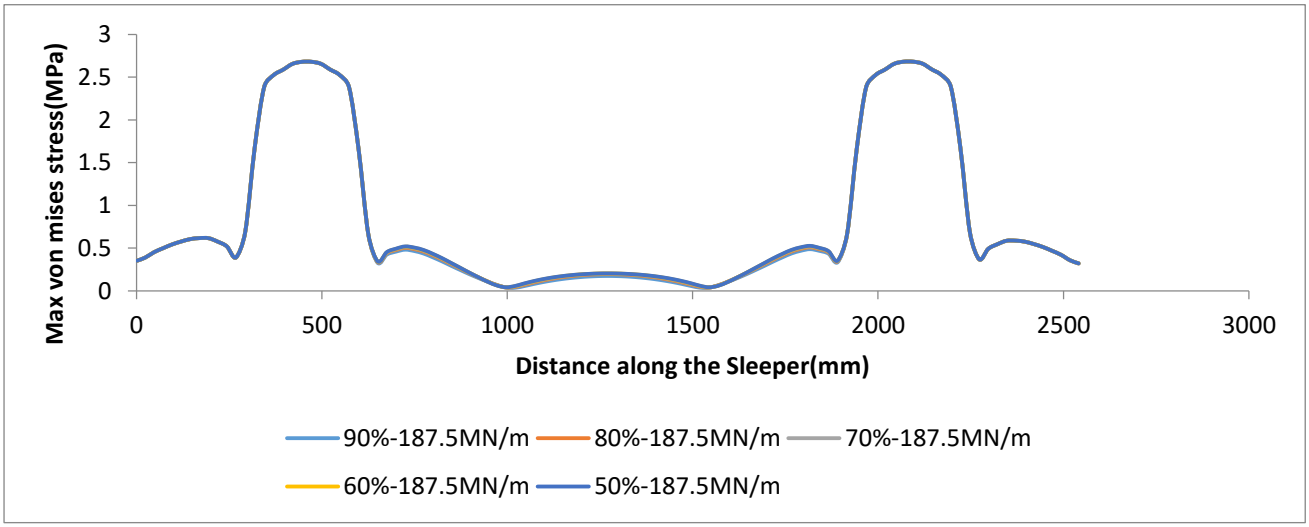

Figure 4.20 Von mises Stress of ballast stiffness variation along the sleeper

It is highlighted with the figure 4.20 that when ballast stiffness reduce at the centre of the sleeper from 100% to 90%,80%.70%,60%, and 50%, supported , the von mises stress of the sleeper increased a small portion more than 100% supported ,therefore this reduction will not cause too much stress on the sleeper.

Shear stress

When a force applied parallel or tangentially to a surface plane or cross sectional area develops shear stress in the material. This force may the result of directly applied loads parallel to an area, or more commonly as the result of bending moments, obliquely applied loads, or other unbalanced forces. As it is shown in the following Figure 4.21

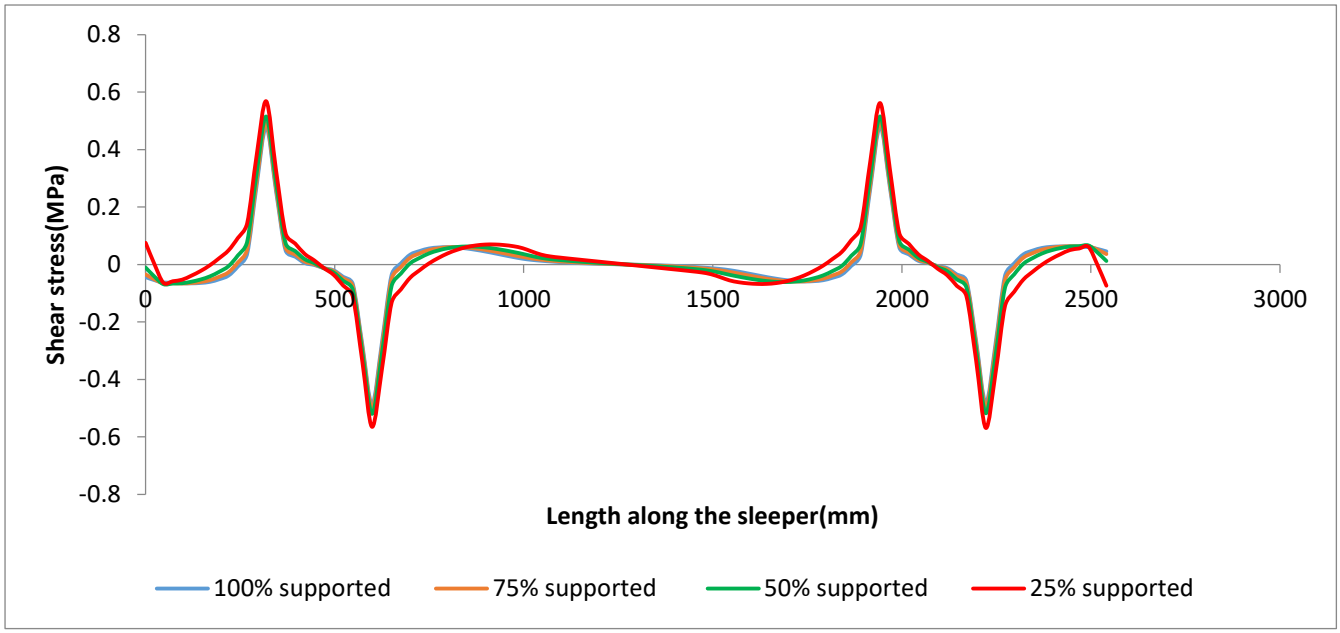

Figure 4.21 Shear stress of ballast stiffness variation along the sleeper

It is highlighted with the figure 4.21 that when ballast stiffness reduce along the sleeper of the sleeper from 100% (full supported) to 75%, 50% and 25 %, supported , the shear stress of the sleeper increased with 2.67%, 6.79%, and 16.87% respectively more than 100% supported ,therefore this reduction will not cause too much stress on the sleeper but it is shown that as the ballast stiffness continues to reduce more stress may occur .

Bending moment

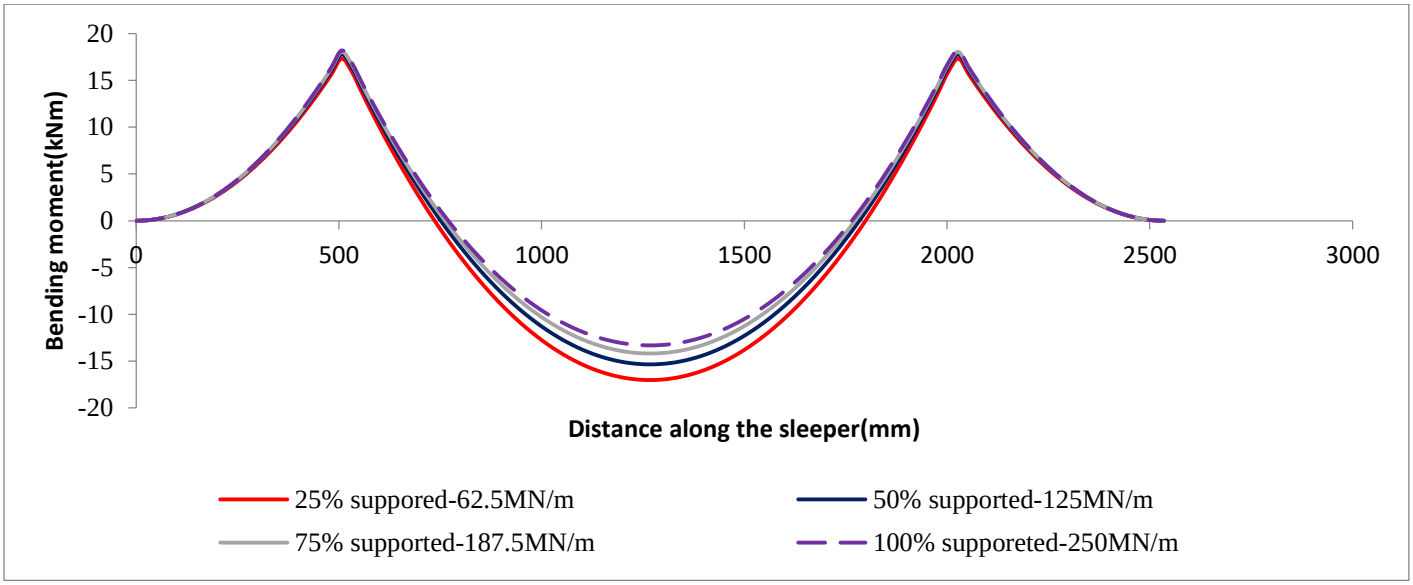

Figure 4.22 Bending moment distribution along the sleeper

Table 4.8 Incremental percentage for maximum bending moment with ballast stiffness reduction

Support condition	Maximum bending moment(kNm)		Incremental percentage (%)	
	RAILSEAT(MR+)	CENTER (MR-)	RAIL SEAT	CENTER
Full supported(250MN/m)	18.2	13.3	0	0
75% supported(187.5MN/)	18	14.2	-0.99	6.76
`50% supported(125MN/m)	17.8	15	-2.2	12.8
25% supported(62.5MN/m)	17.3	16.7	-4.9	25.6

The figure 4.22 shows that there is no significant variation of bending moment once ballast stiffness reduced from 100% supported to 75%,50% and 25% supported . Table 4.8 shows that there is a de-creasing of bending moment at rail seat with 0.99%, 2.2% and 4.9% respectively and it shows that there is increasing of bending moment at the center of sleeper as ballast stiffness reduces 6.76%, 12.8% and 25.6 respectively .

Table 4.9 Summary of over all static analysis results

Description		RAIL SEAT			CENTER SECTION			END SECTION		
No	SUPPORT CONDI-TIONS	Dispace-ment(mm)	Max von mises stress(MPa)	Shear stress(MPa)	Displace-place-ment((mm)	Von mises stress(MPa)	Shear stress(MPa)	Displace-ment(mm)	Von mises stress(MPa)	Shear stress(MPa)
1	K2=0.1KS	0.025338	2.68	0.51873	0.01106	0.0306	0.05564	0.00064	0.35029	-0.03668
2	K2=0.2KS	0.025328	2.68071	0.51608	0.01083	0.03017	0.05863	0.00069	0.38752	-0.03522
3	K2=0.3KS	0.025324	2.68074	0.51254	0.00989	0.05129	0.05924	0.00068	0.66423	-0.03247
4	K2=0.4KS	0.025321	2.68077	0.50758	0.00878	0.03244	0.05721	0.00035	0.34881	-0.0263
5	K2=0.5KS	0.025320	2.68082	0.59993	0.00491	0.05531	0.05357	0.00041	0.45997	-0.03668
6	K2=0.6KS	0.025319	2.68087	0.59994	0.00865	0.02989	0.04855	0.00041	0.50143	-0.0356
7	K2=0.7KS	0.025318	2.68096	0.59995	0.00983	0.02795	0.04279	0.00041	0.52837	-0.0362
8	K2=0.8KS	0.025317	2.68109	0.59995	0.01024	0.03167	0.03658	0.00041	0.51508	-0.03654
9	K2=0.9KS	0.025316	2.68132	0.59996	0.01083	0.02833	0.03038	0.00041	0.48717	-0.03676
10	K2=1KS	0.025315	2.68186	0.59726	0.00318	0.04368	0.02444	0.00046	0.44203	-0.03179
11	100% supported	0.025338	2.68	0.59728	0.0097	0.07018	0.01936	0.00047	0.3904	0.00521
12	80% supported	0.026145	2.68742	0.59729	0.00781	0.03921	0.01563	0.00047	0.33176	0.03706
13	70% supporeted	0.027164	2.70315	0.5973	0.00984	0.02909	0.01287	0.00047	0.2721	-0.03489
14	60%supported	0.028449	2.70846	0.5973	0.01004	0.04141	0.0106	0.00047	0.21134	-0.03518
15	50% supported	0.030121	2.73133	0.51249	-0.0008	0.06506	0.00871	0.00067	0.15353	-0.02659
16	25% supported	0.044737	2.76369	0.59374	0.0051	0.3985	0.00707	0.00049	0.0993	-0.03006
18	100%center stiffness re-duction(187.5MN/m)	0.027750	2.67989	0.47650	0.0059	0.2547	0.00563	0.00044	0.43714	0.0 329
19	90%center stiffness re-duction(187.5MN/m)	0.027770	2.767993	0.45760	0.0032	0.0456	0.00433	0.00046	0.04433	0.0297
20	80%center stiffness re-duction(187.5MN/m)	0.027780	2.68014	0.45758	0.0045	0.0235	0.01165	0.00047	0.68961	0.023

21	70%center stiffness reduction(187.5MN/m)	0.027783	2.68041	0.45775	0.00817	0.02344	0.00206	0.00049	0.35093	-0.03179
22	60%center stiffness reduction(187.5MN/m)	0.027789	2.68115	0.45778	0.0075	0.02347	0.05564	0.00501	0.47133	-0.03122
23	50%center stiffness reduction(187.5MN/m)	0.027804	2.68120	0.46375	0.00932	0.02996	0.05863	0.00049	0.5421	-0.03219
24	100%center stiffness reduction(125MN/m)	0.032100	2.76183	0.50759	-0.0098	0.08079	0.05924	0.00302	0.60318	-0.01685
25	90%center stiffness reduction(125MN/m)	0.032300	2.76185	0.50768	0.00592	0.0396	0.05721	0.00034	0.62476	-0.02474
26	80%center stiffness reduction(125MN/m)	0.032410	2.76242	0.50787	0.00246	0.05125	0.05357	0.00036	0.63173	-0.02296
27	70%center stiffness reduction(125MN/m)	0.032415	2.76286	0.50788	0.00457	0.0429	0.04855	0.00037	0.62076	-0.02404
28	60%center stiffness reduction(125MN/m)	0.032425	2.76378	0.50858	0.00592	0.05962	0.04279	0.00037	0.60159	-0.02474
29	50%center stiffness reduction(125MN/m)	0.032450	2.7663	0.5178	0.00603	0.0599	0.5178	0.0004	0.57026	-0.02477

Chapter 5: CONCLUSION AND RECOMMENDATION

5.1 Conclusion

This study has focused on flexural analysis of monoblock prestressed concrete sleeper where 2 softwares Polybeam that used fixed support and Beam on Elastic Foundation (BOEF) that used elastic foundation have been used to find the maximum bending moments ,shear forces and maximum deflections when a load is externally applied. A 3D solid monoblock prestressed concrete was also used for simulation using ABAQUS and Microsoft Excel was used for the results analysis.

From flexural analysis, at the rail seat the results have shown that the maximum bending from Polybeam and maximum bending moment from BOEF the percentage difference is 0.19% and at the center of the sleeper the maximum bending moment from BOEF and maximum bending moment from Polybeam the percentage difference is 5.12%. The maximum shear force at rail seat the results have shown that maximum shear force from BOEF and maximum shear force from Polybeam are similar because the percentage difference is 0.01%.For deflections for rail seat and at the center of the sleeper the results have shown that the percentage difference is 4.9% and 5.47% respectively. Therefore there is a small portion of difference between results from Polybeam and BOEF.

From static modeling, the possible favorable and unfavorable elastic support circumstances have been analyzed. With a lot of variance in ballast rigidity and very soft support underneath the center of the sleeper and along the length of the sleeper, for all circumstances the results show that the displacements and stresses are significant on the rail seat and it has shown that once ballast stiffness reduce at the centre of the sleeper from 100% to 90%,80%.70%,60%,50%,40%.30%, 20%, and 10% supported , the displacement of the sleeper increased a small portion of (0.004%-0.091%) more than 100% supported and stresses increased(0.027%-0.07%) more than 100% supported. Therefore, once the ballast stiffness reduces at the center of the sleeper there is a small increase in displacement and stresses but to keep the performance of the sleeper, the low ballast stiffness at the center of the sleeper should be avoided.

Once the ballast stiffness reduce along the sleeper from 100% supported (full supported) to 90% , 80%, 70%, 60%,50% and 25% supported , the displacement increased with 3.27%, 7.29%, 12.37%, 18.97%, 27.94% and 76.7% respectively more than full supported and von mises stresses increase with 0.28%, 0.86%, 1.06%, 1.062%, 3.12% and 12.04% respectively more than 100% supported . Therefore, when there is high ballast stiffness reduction along the sleeper, there is more increasing in displacement. Because it is impossible to predict the exact support distribution due to the gradual change in ballast distribution caused by wear and tear, it is of importance for sleeper designers and manufacturers to evaluate the influence of variations in ballast stiffness and distribution.

5.2 Recommendation

Given that railway Sleepers and ballast are two most important components of railway tracks, it is obvious that this segment of the railway system should be thoroughly examined and controlled. So, the investigation of ballast gradation is essential, and must be conducted in the scope of field and laboratory tests.

Additional research could be conducted to study performance of prestressed concrete sleepers by studying their strength and serviceability. Based on field measurements, also other research could be conducted to study the performance of concrete sleepers with various ballast stiffness under dynamic loading by considering all substructure component like sub ballast and subgrade.

REFERENCES

[1] M. D. L, “Analysis of the influence of cracked sleepers under static loading on ballasted railway tracks,” *Sci. World J.*, vol. 2014, p. 10, 2014.

[2] Ruilin you, “Fatigue life assessment method for prestressed concrete sleepers,” *Front. Built Environ.*, vol. 3, no. November, pp. 1–13, 2017.

[3] F. Rezaie, “Experimental and numerical studies of longitudinal crack control for pre-stressed concrete sleepers,” *Eng. Fail. Anal.*, vol. 26, pp. 21–30, 2012.

[4] Y. Panga, “Measurement of deformation of the concrete sleepers under different support conditions using non-contact laser speckle imaging sensor,” *Eng. Struct.*, vol. 205, no. April 2019, p. 110054, 2020, [Online]. Available: https://doi.org/10.1016/j.engstruct.2019.110054.

[5] S. A. Mosayebi, J. A. Zakeri, and M. Esmaeili, “Effects of train bogie patterns on the mechanical performance of ballasted railway tracks with unsupported sleepers,” *Proc. Inst. Mech. Eng. Part F J. Rail Rapid Transit*, vol. 232, no. 1, pp. 238–248, 2018, doi: 10.1177/0954409716664932.

[6] Iara Silva, “Recovery of Cracks in Concrete Railroad Sleepers: Procedure and Case Study,” *Procedia Struct. Integr.*, vol. 11, pp. 130–137, 2018, [Online]. Available: https://doi.org/10.1016/j.prostr.2018.11.018.

[7] S. Kaewunruen, “Investigations of static and dynamic performance of railway prestressed concrete sleepers,” *Proc. SEM Annu. Conf. Expo. Exp. Appl. Mech. 2007*, vol. 1, pp. 110–120, 2007.

[8] J. Sadeghi and P. Barati, “Improvements of conventional methods in railway track analysis and design,” *Can. J. Civ. Eng.*, vol. 37, no. 5, pp. 675–683, 2010, doi: 10.1139/L10-010.

[9] M. A. Sayeed and M. A. Shahin, “Design of ballasted railway track foundations using numerical modelling. Part I: Development1,” *Can. Geotech. J.*, vol. 55, no. 3, pp. 353–368, 2018.

[10] et al. Taufan Abadi, “Improving the performance of railway tracks through ballast interventions,” *Proc. Inst. Mech. Eng. Part F J. Rail Rapid Transit*, vol. 232, no. 2, pp. 337–355, 2018, doi: 10.1177/0954409716671545.

[11] S. Kaewunruen, “Dynamic resistance and rational design of railway prestressed concrete sleepers,” *Proc. fib Symp. 2019 Concr. - Innov. Mater. Des. Struct.*, pp. 1477–1484, 2019.

[12] L. G. Tesso, “Analytical and finite element analysis of rail deflection and bending stress under different sleeper spacing,” ADDIS ABABA UNIVERSITY, 2017.

[13] J. A. Sainz-Aja, “Influence of the operational conditions on static and dynamic stiffness of rail pads,” *Mech. Mater.*, vol. 148, no. May, 2020.

[14] J.-A. Zakeri, “Failures of Railway Concrete Sleepers During Service Life,” *Int. J. Constr. Eng. Manag.*, vol. 1, no. 1, pp. 1–5, 2012.

[15] G. Jing, “Ballast degradation: Effect of particle size and shape using Los Angeles Abrasion test and image analysis,” *Constr. Build. Mater.*, vol. 169, pp. 414–424, 2018.

[16] Yan Wang, “Permeability and Direct Shear Tests Characteristics of Railway Subballast,” *Open Civ. Eng. J.*, vol. 9, no. 1, pp. 388–393, 2015.

[17] E. Kassa, “Railway Track Engineering REGM 6102,” 2018.

[18] B. Lemma, “Analysis on the Influence of Rail Pad on Ballasted Railway Track,” Addis Ababa University, 2018.

[19] Rajesh Gupta and P.K. Bharti, “Evaluation of Wheel Load Lateral Forces using Lateral Vertical Force Measurement Wheel in Dynamic Condition at Rail Wheel Contact Point,” *Int. J. Eng. Res.*, vol. V4, no. 04, pp. 894–902, 2015.

[20] L.-H. Tran, “Influences of Lateral wheel Loads on the Sleeper responses of a Railway Track,” 2020.

[21] T. C. Abadi, “Effect of Sleeper and Ballast Interventions on Rail Track Performance,” University of Southampton, 2015.

[22] J. A. Zakeri, “Lateral Resistance of Railway Track,” no. March 2012, 2014, doi: 10.5772/35421.

[23] W. Koc and A. Wilk, “Investigations of methods to measure longitudinal forces in continuous welded rail tracks using the,” vol. 223, pp. 61–73, 2009.

[24] B. Aursudkij, “A Laboratory Study of Railway Ballast Behaviour under Traffic Loading and Tamping Maintenance,” The University of Nottingham, 2007.

[25] W. Ferdous and A. Manalo, “Failures of mainline railway sleepers and suggested remedies - Review of current practice,” *Eng. Fail. Anal.*, vol. 44, no. September, pp. 17–35, 2014.

[26] E. Gal and R. Kryvoruk, *Properties of concrete*. 2010.

[27] A. Remennikov, “Experimental and Numerical Studies of Railway Prestressed Concrete Sleepers Under Static and Impact Loads,” pp. 25–28, 2007.

[28] “Eurocode 2,” in *Design of concrete structures - Part 1-1 : General rules and rules for buildings Eurocode*, vol. 1, no. 2004, 2011.

[29] J. C. Walraven, “Eurocode 2 : Design of concrete structures,” 2008.

[30] L. Shan, “Railway Sleeper Modelling with Deterministic and Non-deterministic Support Conditions Master Degree Project,” Royal Institute of Technology, 2012.

[31] C. Ngamkhanong, D. Li, and S. Kaewunruen, “Impact capacity reduction in railway prestressed concrete sleepers with vertical holes,” *IOP Conf. Ser. Mater. Sci. Eng.*, vol. 236, no. 1, 2017.

[32] S. Kaewunruen, “Damage and failure modes of railway prestressed concrete sleepers with holes/web openings subject to impact loading conditions,” *Eng. Struct.*, vol. 176, no. March, pp. 840–848, 2018.

[33] D. Li, “Time-Dependent Topology of Railway Prestressed Concrete Sleepers,” *IOP Conf. Ser. Mater. Sci. Eng.*, vol. 245, no. 3, 2017, doi: 10.1088/1757-899X/245/3/032046.

[34] D. Fisseha, “Analysis and Design of Pre-Stressed Concrete Sleepers,” Addis Ababa University, 2001.

[35] “Design of Prestressed Concrete Sleeper Based on Ultimate Limit State Approach,” Addis Ababa University, 2017.

[36] Civil -Railway Airport harbour EWngineering, “Manufacture of concrete sleepers,” in *Manufacture of concrete sleepers*, 2017.

[37] M. Mulugeta, “African Railway Center of Excellence Railway Systems Engineering Introduction System Engineering Permanent Infrastructure Track Geometry.”

[38] *Railway Track Engineering*, vol. 7, no. 3. 2020.

[39] M. Byfield, “Limit state design,” *Struct. Des. from First Princ.*, no. 1, pp. 1–10, 2018, doi: 10.1201/9781315116914-1.

[40] M. Murray, “Ultimate limit states design of concrete railway sleepers,” no. February, 2015, doi: 10.1680/tran.10.00048.

[41] B. Bae, H. Choi, and C. Choi, “Flexural Strength Evaluation of Reinforced Concrete Members

with Ultra High Performance Concrete," vol. 2016, 2016.

[42] Cambridge, "Fatigue Limit-State Design," in *Fatigue Limit-State Design*, 2018.

[43] S. Kaewunruen, A. M. Remennikov, and M. H. Murray, "Limit states design of railway concrete sleepers," *Proc. Inst. Civ. Eng. Transp.*, vol. 165, no. 2, pp. 81–85, 2012.

[44] H. E. Wolf, J. R. Edwards, M. S. Dersch, and C. P. L. Barkan, "Flexural Analysis of Prestressed Concrete Monoblock Sleepers for Heavy-Haul Applications : Methodologies and Sensitivity To Support Conditions," *IHHA 2015 Conf.*, no. June 2015, 2015.

[45] A. M. Remennikov and S. Kaewunruen, "Resistance of Railway Concrete Sleepers to Impact Loading," in *The 7th International Conference on Shock and Impact Loads on Structures*, 2007, no. October, pp. 489–496, [Online]. Available: www.uow.edu.au.

[46] W. Ferdous and A. Manalo, "Failures of mainline railway sleepers and suggested remedies - Review of current practice," *Eng. Fail. Anal.*, vol. 44, no. April 2020, pp. 17–35, 2014, doi: 10.1016/j.engfailanal.2014.04.020.

[47] R. G. Kernes, A. A. Shurpali, J. R. Edwards, M. S. Dersch, D. A. Lange, and C. P. L. Barkan, "Investigation of the mechanics of rail seat deterioration and methods to improve the abrasion resistance of concrete sleeper rail seats," *Proc. Inst. Mech. Eng. Part F J. Rail Rapid Transit*, vol. 228, no. 6, pp. 581–589, 2014, doi: 10.1177/0954409714530911.

[48] O. of Research, Development, A. Technology, and D. 20590 Washington, "Detection of Concrete Tie Rail Seat Deterioration," no. September, 2019.

[49] R. H. Lutch, D. K. Harris, and T. M. Ahlborn, "Causes and preventative methods for rail seat abrasion in North America's railroads," *Proc. Int. Conf. Cold Reg. Eng.*, vol. 41072, no. October, pp. 455–466, 2009, doi: 10.1061/41072(359)44.

[50] J. Zakeri and F. H. Rezvani, "Failures of Railway Concrete Sleepers During Service Life," *Int. J. Constr. Eng. Manag.*, vol. 1, no. 1, pp. 1–5, 2012, doi: 10.5923/j.ijcem.20120101.01.

[51] J. Donaire-Ávila, A. Montañés-López, and F. Suárez, "Influence of temperature on the longitudinal cracking in multipurpose precast concrete sleepers prior to their installation," *Materials (Basel).*, vol. 12, no. 7, pp. 9–11, 2019, doi: 10.3390/ma12172731.

[52] J. Taherinezhad, "A review of behaviour of Prestressed concrete sleepers," *Electron. J. Struct. Eng.*, vol. 13, no. 1, pp. 1–16, 2013.

[53] M. Mulugeta, "ADDIS ABABA INSTITUTE OF TECHNOLOGY SCHOOL OF CIVIL

AND ENVIRONMENTAL ENGINEERING RAIL CRACK ANALYSIS WITH INSPECTION AND MAINTENANCE PLAN AT TRANSITION SECTION BETWEEN BRIDGES AND EMBANKMENTS A Thesis in Railway Civil Engineering," Addis Ababa University, 2016.

[54] S. Kaewunruen and A. M. Remennikov, "Dynamic Crack Propagations in Prestressed Concrete Sleepers in Railway Track Systems Subjected to Severe Impact Loads," no. June, pp. 749–754, 2010.

[55] N. Theogene, "Optimization of concrete sleepers subjected to static and impact loadings," Addis Ababa University, 2019.

[56] R. H. Lutch, "Digital Commons @ Michigan Tech Capacity optimization of a prestressed concrete railroad tie OF," 2009.

[57] J. A. Zakeri and J. Sadeghi, "Field investigation on load distribution and deflections of railway track sleepers," *J. Mech. Sci. Technol.*, vol. 21, no. 12, pp. 1948–1956, 2007, doi: 10.1007/BF03177452.

[58] M. Kebede, "Flexural Performance Evaluation of different Countries Concrete Sleepers for the case of Ethiopian Railway Track Design," Addis Ababa University, 2015.

[59] S. Kaewunruen and A. Remennikov, "Rotational capacity of railway prestressed concrete sleeper under static hogging moment," pp. 5–8, 2006.

[60] H. Feng, "3D - models of Railway Track for dynamic Analysis," *KTH, Sch. Archit. Built Environ. (ABE), Transp. Sci.*, vol. M,Sc, p. 92, 2011, [Online]. Available: http://urn.kb.se/resolve?urn=urn:nbn:se:kth:diva-52619.

[61] J. Taherinezhad, M. Sofi, P. A. Mendis, and T. Ngo, "A review of behaviour of Prestressed concrete sleepers," *Electron. J. Struct. Eng.*, vol. 13, no. 1, pp. 1–16, 2013.

[62] J. P. Srivastava, P. K. Sarkar, and V. Ranjan, "Static analysis of railway track," no. March 2017, pp. 1–13, 2015.

[63] W. C. Young and R. G. Budynas, *Roark ' s Formulas for Stress and Strain*. .

[64] M. Sol-sánchez, F. Moreno-navarro, and M. C. Rubio-gámez, "The use of elastic elements in railway tracks : A state of the art review," vol. 75, pp. 293–305, 2015, doi: 10.1016/j.conbuildmat.2014.11.027.

[65] J. Sadeghi, A. hasheminezhad, and M. Essmayil Kaboli, "Investigation of the Influences of

Track Superstructure Parameters on Ballasted Railway Track Design," *Civ. Eng. Infrastructures J. (Journal Fac. Eng.*, vol. 48, no. 1, pp. 157–174, 2015, doi: 10.7508/ceij.2015.01.011.

[66] S. Kaewunruen, E. K. Gamage, and A. M. Remennikov, "Modelling Railway Prestressed Concrete Sleepers (Crossties) with Holes and Web Openings," *Procedia Eng.*, vol. 161, no. June 2017, pp. 1240–1246, 2016, doi: 10.1016/j.proeng.2016.08.556.

[67] S. Kaewunruen and A. M. Remennikov, "Experimental and Numerical Studies of Railway Prestressed Concrete Sleepers Under Static and Impact Loads," *Civ. Comput.*, no. January, pp. 25–28, 2007.

[68] Australian Standard, "Raiway Track Material Part 14: Prestressed Concrete Sleepers," 2019.

[69] N. Theogene, "Optimization of Concrete Sleepers Subjected To Static and Impact," Addis Ababa University, 2019.

[70] R. Gustavson, "Static and Dynamic Finite Element Analyses of Concrete Sleepers," pp. 49–66, 2000.

[71] C. Library and O. F. Jsce, "A STUDY ON LIMIT-STATE DESIGN METHOD FOR PRESTRESSED CONCRETE SLEEPERS (Translation from Proceedings of JSCE, No.557/V-34, February 1997)," no. 33, 1999.